Department of Applied Physics

Theory and models for Monte Carlo simulations of minority particle populations in tokamak plasmas

Eero Hirvijoki

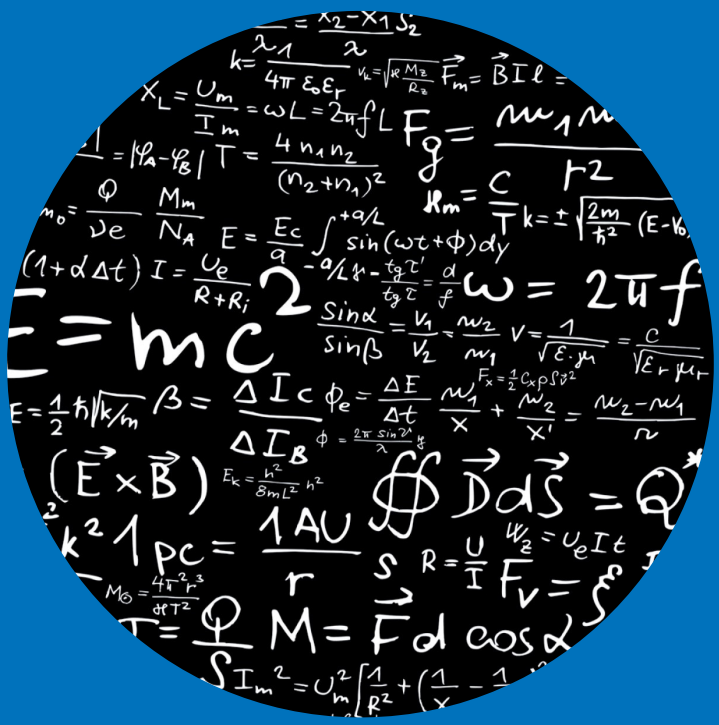

Aalto University

DOCTORAL DISSERTATIONS

Aalto University publication series
DOCTORAL DISSERTATIONS 16/2014

Theory and models for Monte Carlo simulations of minority particle populations in tokamak plasmas

Eero Hirvijoki

A doctoral dissertation completed for the degree of Doctor of Science to be defended, with the permission of the Aalto University School of Science, at a public examination held at the lecture hall E in the main building of the school on 20 March 2013 at 13.

Aalto University
School of Science
Department of Applied Physics
Fusion

Supervising professor
Prof. Rainer Salomaa, Aalto University, Finland

Thesis advisor
Prof. Taina Kurki-Suonio, Aalto University, Finland

Preliminary examiners
Prof. Karl Lackner, Max Planck Institüt für Plasma Physik, Germany
Prof. Yves Peysson, Commissariat à l'Energie Atomique et aux Energies Alternatives, France

Opponent
Prof. Per Helander, Max Planck Institut für Plasma Physik, Germany

Aalto University publication series
DOCTORAL DISSERTATIONS 16/2014

ISBN 978-952-60-5559-6
ISBN 978-952-60-5560-2 (pdf)
ISSN-L 1799-4934
ISSN 1799-4934 (printed)
ISSN 1799-4942 (pdf)
http://urn.fi/URN:ISBN:978-952-60-5560-2

Unigrafia Oy
Helsinki 2014

Finland

Publication orders (printed book):
eero.hirvijoki@aalto.fi

Aalto University

Abstract

Aalto University, P.O. Box 11000, FI-00076 Aalto www.aalto.fi

Author
Eero Hirvijoki

Name of the doctoral dissertation
Theory and models for Monte Carlo simulations of minority particle populations in tokamak plasmas

Publisher School of Science

Unit Department of Applied Physics

Series Aalto University publication series DOCTORAL DISSERTATIONS 16/2014

Field of research Plasma physics

Manuscript submitted 5 December 2013 **Date of the defence** 20 March 2014

Permission to publish granted (date) 29 January 2014 **Language** English

☐ **Monograph** ☒ **Article dissertation (summary + original articles)**

Abstract

This thesis presents the essential parts of the first principles theory that is used to describe the evolution of minority particle populations in tokamak plasmas. Also, numerical models specific for Monte Carlo studies of fast ion transport are introduced, and the transport of alpha particles due to magnetohydrodynamical (MHD) activity is investigated in ITER scenarios.

The thesis starts by introducing the very idea behind Monte Carlo simulations: an explicit proof of the connection between a Fokker-Planck equation and stochastic processes is given. This connection is then used to provide the stochastic differential equation for a charged particle that describes both the Hamiltonian and collisional motion of the particle in a plasma. Although following stochastic trajectories of charged particles and constructing the distribution function as a statistical average allows first principle solutions of the corresponding kinetic equation, the method is computationally very expensive. To offer numerically more attractive approach, the theoretical part is continued by introducing the guiding center transformation of the particle kinetic equation. The transformation is discussed in detail, and derivation of the guiding center motion is given explicitly.

The theoretical work and the fast ion specific models are then implemented to construct a revieved version of the numerical Monte Carlo tool called ASCOT. As an application, the code is used to study MHD induced alpha particle transport in ITER. The results for the transport studies confirm that the neoclassical tearing modes would not endanger the integrity of the plasma facing components. However, it is noticed that the transport due to toroidal Alfvén eigenmodes could significantly change the power deposition from the alphas to the bulk plasma.

Keywords Monte Carlo, tokamak, plasma

ISBN (printed) 978-952-60-5559-6 **ISBN (pdf)** 978-952-60-5560-2

ISSN-L 1799-4934 **ISSN (printed)** 1799-4934 **ISSN (pdf)** 1799-4942

Location of publisher Helsinki **Location of printing** Helsinki **Year** 2014

Pages 132 **urn** http://urn.fi/URN:ISBN:978-952-60-5560-2

Aalto-yliopisto

Tiivistelmä

Aalto-yliopisto, PL 11000, 00076 Aalto www.aalto.fi

Tekijä
Eero Hirvijoki

Väitöskirjan nimi
Teoria ja mallit vähemmistöhiukkasten Monte Carlo simulointiin tokamak plasmoissa

Julkaisija Perustieteiden korkeakoulu

Yksikkö Teknillisen fysiikan laitos

Sarja Aalto University publication series DOCTORAL DISSERTATIONS 16/2014

Tutkimusala Plasmafysiikka

Käsikirjoituksen pvm 05.12.2013 **Väitöspäivä** 20.03.2014

Julkaisuluvan myöntämispäivä 29.01.2014 **Kieli** Englanti

☐ **Monografia** ☒ **Yhdistelmäväitöskirja (yhteenveto-osa + erillisartikkelit)**

Tiivistelmä

Tämä väitöstyö kattaa perusteorian, joka kuvaa vähemmistöhiukkasia tokamak plasmoissa. Lisäksi työssä esitetään Monte Carlo malleja nopeiden hiukkasten mallintamiseen ja tuloksia nopeiden alfa hiukkasten simuloinnista ITER tokamakissa.

Jotta Monte Carlo menetelmien käyttö olisi perusteltua, yhteys vähemmistöhiukkasten distribuutiofunktiota kuvaavan Fokker-Planck yhtälön ja stokastisen prosessin välillä todistetaan heti työn aluksi. Yhteyttä hyödyntämällä työssä esitetään stokastinen differentiaaliyhtälö varatulle hiukkaselle huomioiden sekä Hamiltoniaaninen että törmäyksellinen liike. Käytännössä distribuutiofunktion suora ratkaiseminen on kuitenkin numeerisesti erittäin kallista. Tämän vuoksi distribuutiofunkiota kuvaavalle Fokker-Planck yhtälölle suoritetaan muunnos, joka antaa paremmat valmiudet numeeriseen ratkaisuun. Muunnoksen perustana oleva johtokeskusteoria esitään tarkasti välivaiheet sisältäen.

Teoriaa ja laadittuja malleja on myös sovellettu rakentamalla ASCOT-niminen ohjelmakoodi. Koodin avulla nopeiden alfa-hiukkasten kulkeutumista on voitu tutkia ITER tokamakissa aiempaa tarkemmin. Ensimmäistä kertaa tutkimus on voitu tehdä huomioiden sekä plasman aiheuttemat magneettiset epästabiiliudet, että itse tokamak laitteen tuottamat epähomogeeniset muodostumat magneettikentässä.

Avainsanat Monte Carlo, tokamak, plasma

ISBN (painettu) 978-952-60-5559-6 **ISBN (pdf)** 978-952-60-5560-2

ISSN-L 1799-4934 **ISSN (painettu)** 1799-4934 **ISSN (pdf)** 1799-4942

Julkaisupaikka Helsinki **Painopaikka** Helsinki **Vuosi** 2014

Sivumäärä 132 **urn** http://urn.fi/URN:ISBN:978-952-60-5560-2

Preface

This thesis is a culmination of my work in the fusion research group in Aalto University. The very beginning of the journey, that I have now taken, was not quite expected. Starting in 2008 with interviews for a summer trainee positions, all my belongings were stolen during that afternoon. Since then, the road has been mostly uphill.

After I completed the Master's studies during the summer 2010, our group leader Taina somehow managed to protect me from the lure of decent salary the private sector could have offered, and convinced me to continue in fusion research. No regrets on that decision. The group of Antti, Otto, Simppa, Tuomas, Juho, and Seppo, not forgetting my instructor Taina, has offered a reason to keep biking to the office through these years, even if it was -25°C outside. Guys, it's been a pleasure.

I would also like to thank, especially, Prof. Alain Brizard, who has taught me some very cool stuff. Alain and his family also generously offered a warm atmosphere and excellent dinners during my visit in Vermont in November 2012. Professors Rainer Salomaa and Mathias Groth I want to thank for offering an opportunity to work within this research group. Nor should I forget other colleagues in the fourth floor of Kone-builbing in Otaniemi. Last but not least, I thank my girlfriend Sanni and the rest of my family for the support during tougher times.

Espoo, January 31, 2014,

Eero Hirvijoki

Contents

List of Publications

This thesis consists of an overview and of the following publications which are referred to in the text by their Roman numerals.

I E. Hirvijoki and T. Kurki-Suonio. Monte Carlo diffusion operator for anomalous radial transport in tokamaks. *Europhysics Letters*, 97, 5, 55002, March 2012.

II E. Hirvijoki, A. Snicker, T. Korpilo, P. Lauber, E. Poli, M. Schneller, and T. Kurki-Suonio. Alfvén Eigenmodes and Neoclassical tearing modes for orbit-following implementations. *Computer Physics Communications*, 183, 2589-2593, July 2012.

III E. Hirvijoki, A. Brizard, A. Snicker, and T. Kurki-Suonio. Monte Carlo implementation of a guiding-center Fokker-Planck kinetic equation. *Physics of Plasmas*, 20, 9, 092505, September 2013.

IV E. Hirvijoki, O. Asunta, T. Koskela, T. Kurki-Suonio, J. Miettunen, S. Sipilä, A. Snicker, and S. Äkäslompolo. ASCOT: solving the kinetic equation of minority particle species in tokamak plasmas. Accepted for publication in *Computer Physics Communications*, January 2014.

V A. Snicker, E. Hirvijoki, and T. Kurki-Suonio. Power loads to ITER first wall structures due to fusion alphas in a non-axisymmetric magnetic field including the presence of MHD modes. *Nuclear Fusion*, 53, 9, 093028, July 2013.

Author's Contribution

Publication I: "Monte Carlo diffusion operator for anomalous radial transport in tokamaks"

The author derived the model presented in the paper and wrote the manuscript receiving valuable help from the co-author.

Publication II: "Alfvén Eigenmodes and Neoclassical tearing modes for orbit-following implementations"

The author derived the model presented in the paper and implemented it in cooperation with Mr. Snicker. The author also wrote the manuscript in collaboration with the co-authors.

Publication III: "Monte Carlo implementation of a guiding-center Fokker-Planck kinetic equation"

The author derived the results presented in the paper together with Prof. Brizard and wrote the manuscript in collaboration with the co-authors.

Publication IV: "ASCOT: solving the kinetic equation of minority particle species in tokamak plasmas"

The author started the development of the new code presented in the paper. The code was finished when the co-authors joined the effort adding different physics models to the code. The author organized the writing of the manuscript which was finished in collaboration with the co-authors.

Publication V: "Power loads to ITER first wall structures due to fusion alphas in a non-axisymmetric magnetic field including the presence of MHD modes"

The author contributed by implementing the tool for carrying out the numerical studies and by writing the theoretical part of manuscript together with the co-authors.

1. Introduction

The word *plasma* is commonly associated with plasma televisions and blood cells, or understood as some nasty weird goo appearing in the Ghostbusters movie. Within the fusion community the word has a different meaning and it is used to define 99 %, or even more, of the known matter in the universe. Stars, for example, are massive dense plasma balls, and the closest major plasma formation to us is the ionosphere. The name of this dilute layer surrounding the Earth at the edge of the emptiness of space refers to the components of plasma: it consists of charged particles, ions and electrons.

Due to the charged particles the behavior of plasmas greatly differ from that of neutral gases. The charged particles are influenced not only by gravity but also by strong electromagnetic forces. In the Sun these forces are responsible for rapid energetic eruptions of plasma, called solar flares. On the Earth, remnants of these flares can be occasionally seen as the high energy particles escaping the solar corona reach the Earth's magnetic field, get diverted towards the geomagnetic poles, and collide with neutral particles in the upper atmosphere. As a result, a bright light display, called the Auroras, can be seen in the sky.

Thermonuclear fusion of protons and other light nuclei in high temperature and pressure provides the energy for the Sun to maintain these events. Mimicking this energy source on Earth has long been desired by humanity but we do not have the massive gravitational field of the Sun to shape and control the plasma. Fortunately, just like the solar flares get guided towards the Earth's geomagnetic poles, laboratory plasmas can be confined with carefully designed magnetic fields.

In a fusion reactor, there are solar flares as well. These events of rapid bursts of energy, called the Edge Localized Modes or ELMs [1, 2, 3, 4] can, however, cause a great deal of thermal stress to the machine's plasma

facing components (PFCs). Methods to mitigate the ELMs have been investigated and one of the best candidates has turned out to be resonant magnetic perturbations (RMPs) applied to the plasma edge [5, 6]. These perturbations increase the transport at the edge restraining the build-up of the ELMs.

While the external perturbations have beneficial effect on the ELMs, they are anticipated to affect the confinement of energetic particle populations negatively [7, 8, 9, 10]. The energetic particles, though forming only a minority population in the plasma, are crucial as they provide means to heat the plasma to temperatures needed for fusion. Deterioration of their confinement could lead to loss of valuable heating power and, also, to increased heat flux to the PFCs [11, 12, 13]. Thus, any unnecessary loss should be avoided.

The external RMPs provide one example of local aberrations in the magnetic field that cause transport of energetic particles. Another important source responsible for perturbations and transport is the inherent magnetohydrodynamical (MHD) activity [14, 15, 16, 17, 18, 19]. In this thesis, first principle methods to study the minority particle transport are derived and revised, and models specific for energetic particles are developed.

1.1 Thermonuclear fusion

Fusion is possible when two nuclei come sufficiently close to each other so that the Strong force can overcame the repulsive electric force between the nuclei and bind the two into a heavier one. On Earth, the feasible nuclear fusion reactions are those involving hydrogen isotopes deuterium (D) and tritium (T):

$$\mathrm{D} + \mathrm{D} \xrightarrow{50\%} \mathrm{He}^3\ (0.82\ \mathrm{MeV}) + \mathrm{n}\ (2.45\ \mathrm{MeV}), \tag{1.1}$$

$$\mathrm{D} + \mathrm{D} \xrightarrow{50\%} \mathrm{T}\ (1.01\ \mathrm{MeV}) + \mathrm{H}\ (3.02\ \mathrm{MeV}), \tag{1.2}$$

$$\mathrm{D} + \mathrm{T} \rightarrow \mathrm{He}^4\ (3.5\ \mathrm{MeV}) + \mathrm{n}\ (14.1\ \mathrm{MeV}), \tag{1.3}$$

$$\mathrm{D} + \mathrm{He}^3 \rightarrow \mathrm{He}^4\ (3.6\ \mathrm{MeV}) + \mathrm{p}\ (14.7\ \mathrm{MeV}). \tag{1.4}$$

The cross sections, $\langle \sigma v \rangle$, measuring the probability for a reaction to occur, are presented in Fig. 1.1. The two possible D-D reaction are presented together. It is seen that fusion reactions are most easily achieved mixing Deuterium and Tritium together, although obtaining maximal fusion yield would still require a temperature of roughly 70 keV.

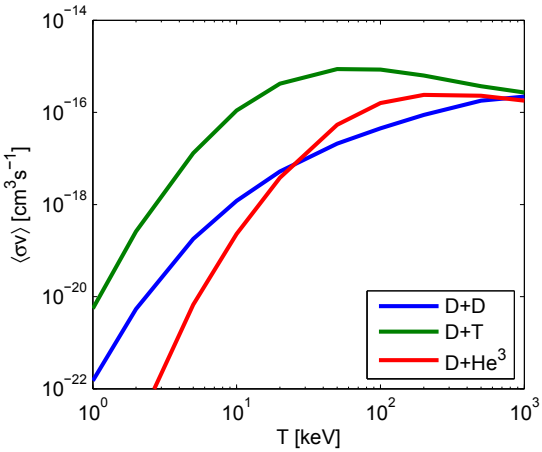

Figure 1.1. Fusion cross sections for reactions considered for energy production on Earth. Data adopted from NRL plasma formulary [20].

As the temperatures to achieve fusion are high, it is desired that the plasma itself would provide enough power to maintain it hot, and excess use of auxiliary heating could be avoided. The Lawson–criterion [21] specifies the conditions for *ignition*, demanding that the losses are overcome by the energy produced in fusion reactions. In a plasma of 50–50 mixture of the fuel, a simplified Lawson–criterion for the density n, temperature T, and energy confinement time τ_E is given by

$$nT\tau_E \geq \frac{12k_B}{E_f}\frac{T^2}{\langle\sigma v\rangle}, \tag{1.5}$$

where E_f is the energy of the fusion products that carry charge (neutrons do not donate energy to the plasma), and k_B is the Boltzmann constant. The triple product $nT\tau_E$ for the three considered reactions are presented in Fig. 1.2. Again, the D-T reaction, achieving the lowest value, is seen the most attractive option. The minimum value, obtained at T=13 keV, however, still is 1000 times larger than the energy required to detach an electron from a hydrogen atom.

Keeping the plasma confined at such temperature for long enough is by no means a trivial task. The options are limited to either isolating the plasma from its surroundings with a magnetic field, or maximizing the density so that the confinement can be compared to an explosion. In the field of *magnetic confinement*, the current flagship concept is the *tokamak*.

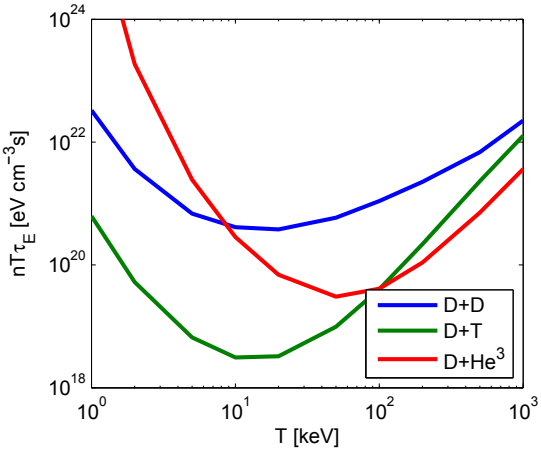

Figure 1.2. The Lawson's triple product criterion for fusion reactions considered for energy production on Earth. Data adopted from NRL plasma formulary [20].

1.2 The tokamak and behavior of charged particles therein

In a tokamak, a magnetic field is exploited to guide the charged particles and to keep them confined within a torus shaped volume. The main component of the magnetic field is toroidal, generated with external coils. A transformer circuit in the center of the tokamak is used to induce a toroidal current into the plasma, eventually creating also a so-called poloidal magnetic field. The internal poloidal field, together with the external toroidal component, confines the plasma, and the strength and shape of the field is determined by balancing the magnetic and kinetic forces according to the equation

$$\nabla p = \mathbf{j} \times \mathbf{B}, \tag{1.6}$$

where p is the plasma pressure, $\mathbf{j}$ is the electric current density, and $\mathbf{B}$ is the magnetic field. A schematic view of the magnetic configuration in a tokamak is presented in Fig. 1.3.

From Fig. 1.3 one sees that the toroidal field coils are relatively tightly packed and, thus, in the first approximation to solve the force-balance equation, the magnetic ripple caused by a finite number of the toroidal field coils is neglected. As a result, the simplified magnetic geometry of a tokamak can be expressed in terms of one *axisymmetric* flux function, ψ, and the magnetic field is given by [22]

$$\mathbf{B} = g(\psi)\nabla\phi + \nabla\phi \times \nabla\psi, \tag{1.7}$$

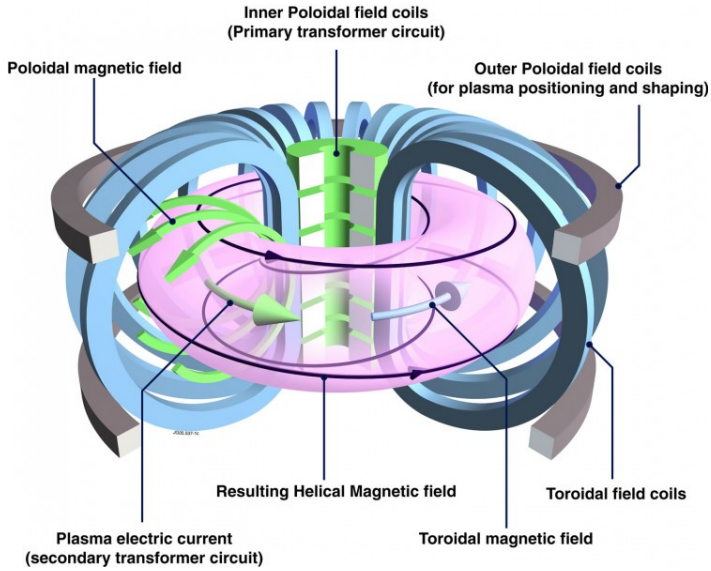

Figure 1.3. A simplified presentation of the tokamak configuration. Courtesy of EFDA.

where ϕ stands for to the toroidal angle, and $g\nabla\phi$ is the total toroidal field including the effect of the plasma.

In this axisymmetric configuration the collisionless particle orbits are well defined and, when projected onto a poloidal plane, the orbits form closed contours as illustrated in Fig. 1.4. In the absence of time-dependent electric and magnetic fields, the poloidal projection of the particle orbit will be broken only because of Coulomb collisions. The collisions change the particle velocity space coordinates and can be interpreted as jumps between different collisionless orbit topologies. This immediately suggests one approach to describe the collisional transport: to follow the time development of the orbits, not the actual particles. This procedure, called the *orbit-averaging* [23, 24, 25, 26, 27, 28] reduces the dimensionality of the problem and, instead of the full six-dimensional phase space $(\mathbf{x}, \mathbf{v})$, three coordinates are enough to describe the evolution of an orbit.

Despite of offering a huge computational benefit when studying minority particle confinement, the orbit-averaged descriptions of collisional transport suffer from the loss of applicability. From Figure 1.4 it is evident that the coordinate ψ, often used as one of the three coordinates in orbit-averaged methods, does not describe well all the orbits. Also, the beautiful assumption of axisymmetry, required in orbit-averaging, can be severely compromised, and not only because of the toroidal ripple. In ITER, e.g., the test modules for tritium breeding (TBMs) and the neutral

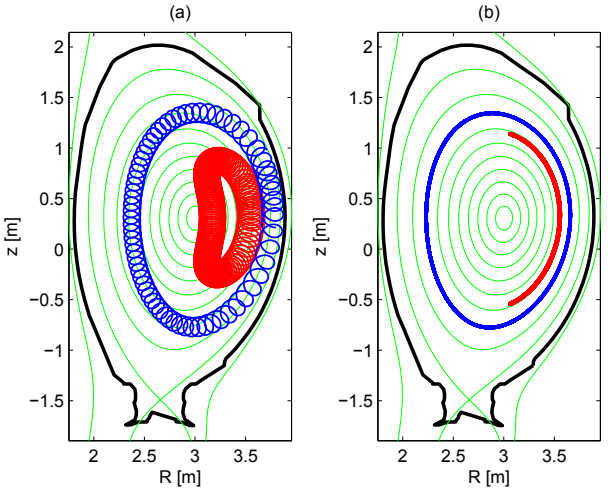

Figure 1.4. Poloidal projections of typical orbit topologies in a Tokamak with an axisymmetric magnetic field. On the left (a), orbit of a passing (blue) and a trapped (red) 3.5 MeV alpha particle. On the right (b), orbit of a passing (blue) and a trapped (red) 3 keV Carbon. Note the completely different trajectories and deviations from the flux surfaces (light green, ψ). The machine wall is presented by the black broken line.

beam injectors (NBIs) for auxiliary heating and current drive will perturb the magnetic field far from axisymmetry. Furthermore, the orbit-averaged description of collisional transport is limited to regions of closed flux surfaces and, as impurities migrate to the plasma from the wall, which is in contact with the open flux surfaces, more flexible method is needed.

In this thesis the power of *non-canonical Hamiltonian guiding center formalism* [29, 30, 31, 32, 33] is harnessed to overcome the limitations of the orbit-averaged methods. Although many other variations of the guiding center theory exist [34, 35, 36, 37, 38, 39], the non-canonical Hamiltonian approach has proven itself the most useful one considering practical applications. The theory inherently adapts to various 3D effects, is not restricted to closed flux-surfaces, can describe all different orbit topologies, and expresses the motion in terms of measurable quantities. The power of the method is that it describes the essential parts of the particle motion along the orbit while making the rapid gyrating motion around the magnetic field line redundant. The only limitation of the theory is that the particle's Larmor radius has to be small compared to the gradient lengths of the background electromagnetic fields, and that the fields do not change rapidly in time compared to the particle's gyration frequency (the Larmor radius is $\rho = v_\perp/\Omega$, where $v_\perp$ is the velocity perpendicular

to the magnetic field and the gyration frequency is $\Omega = qB/m$ where B is the magnetic field strength, q is the charge and m is the mass of the particle). Although the five remaining phase space coordinates needed for describing the guiding center motion is more than the three required in orbit-averaged describtion, the computational cost for studying transport is still significantly reduced compared to the fully described particle motion.

1.3 Organization of the thesis

This thesis presents the essential parts of the theory that is used to describe the evolution of minority particle populations in tokamak plasmas. The thesis starts by introducing the very idea behind Monte Carlo simulations: a connection between Fokker-Planck equation and stochastic processes is established in Chapter 2. As an example, the theory is applied to the charged particle kinetic equation and a method is offered to solve the kinetic equation in terms of stochastic differential equations. In Chapter 3, the theoretical basis is extended to the guiding center formalism. An explicit derivation of the Hamiltonian guiding center motion is presented using the Lie-transform theory, and the details leading the to collisional guiding center motion are presented by elaborating the results derived in Ref. [40] and in Publication III. In Chapter 4, additional models, specific for fast ion transport calculations, are summarized from the Publications I and II and a tool for minority particle simulations, developed in Publication IV, is described. Finally, the methods presented in this thesis are used to study fusion born alpha particles in ITER, and the main results from Publication V are presented.

2. Basics of kinetic theory

As distribution function contains all information of the system at hand, transport can be described in terms of it. Macroscopic quantities, e.g., density, pressure, and momentum, are be obtained as velocity space moments of the distribution function, and the changes in the energy and momentum are obtained as moments of the equation that describes the time evolution of the distribution function. In this chapter the distribution function for minority species is established assuming that the background plasma is not changed radically due to the presence of the minority population.

2.1 Derivation of the kinetic Fokker-Planck equation

In plasmas, the particles are in constant motion causing microscopic fluctuations in the electromagnetic fields and every particle in the system feels the fluctuations caused by the others. Exact description of such a many-body-problem is impossible, as it would require the exact motion of each particle involved. Since the motion of a particle in a fluctuating electromagnetic field resembles that of Brownian motion, it is not even necessary to describe the problem exactly. The electric field fluctuations can be described in terms of fluctuation spectrum and dielectric response function, and the average effect of the fluctuations on the particle motion can be calculated. The particle motion in the phase space due to the fluctuations can then be ideally considered as a step-like Markov process driven by *Coulomb collisions*, and a probabilistic view adopted.

Although the collisions are inherently described at the particle level, they can be included into the time evolution of a distribution function. Let τ denote a small time interval during which the particle position $\mathbf{z}$ changes by a random amount Δ. Then, the probability density $f(\mathbf{z}, t + \tau)$

for finding the particle at $\mathbf{z}$ after the time τ has passed is obtained as a weighted sum over different possible jumps

$$f(\mathbf{z}, t+\tau) = \int d\Delta \; f(\mathbf{z}-\Delta, t) W_\tau(\mathbf{z}-\Delta, \Delta), \tag{2.1}$$

where $W_\tau(\mathbf{z}, \Delta)$ is the transition probability ($\int W_\tau(\mathbf{z}, \Delta) d\Delta = 1$) for the jump to happen [41].

Expanding both the distribution function and the transition probability in Eq. (2.1) around $\mathbf{z}$ and t

$$\begin{aligned} f(\mathbf{z}, t+\tau) = \int d\Delta \Bigg[& f(\mathbf{z}, t) W_\tau(\mathbf{z}, \Delta) - \frac{\partial}{\partial \mathbf{z}} \left(f(\mathbf{z}, t) W_\tau(\mathbf{z}, \Delta) \right) \cdot \Delta \\ & + \frac{1}{2} \frac{\partial}{\partial \mathbf{z}} \frac{\partial}{\partial \mathbf{z}} \left(f(\mathbf{z}, t) W_\tau(\mathbf{z}, \Delta) \right) : \Delta\Delta + \mathcal{O}(\Delta\Delta\Delta) \Bigg], \end{aligned} \tag{2.2}$$

and defining the integrals

$$\langle \Delta \rangle = \int d\Delta W_\tau(\mathbf{z}, \Delta) \Delta, \tag{2.3}$$

$$\langle \Delta\Delta \rangle = \int d\Delta W_\tau(\mathbf{z}, \Delta) \Delta\Delta, \tag{2.4}$$

$$\langle \Delta\Delta\Delta \rangle = \int d\Delta W_\tau(\mathbf{z}, \Delta) \Delta\Delta\Delta, \tag{2.5}$$

Eq. (2.1) is simplified (after division by the time interval τ) into

$$\begin{aligned} \frac{f(\mathbf{z}, t+\tau) - f(\mathbf{z}, t)}{\tau} = & - \frac{\partial}{\partial \mathbf{z}} \cdot \left(f(\mathbf{z}, t) \frac{\langle \Delta \rangle}{\tau} \right) \\ & + \frac{1}{2} \frac{\partial}{\partial \mathbf{z}} \frac{\partial}{\partial \mathbf{z}} : \left(f(\mathbf{z}, t) \frac{\langle \Delta\Delta \rangle}{\tau} \right) + \mathcal{O}(\frac{\langle \Delta\Delta\Delta \rangle}{\tau}). \end{aligned} \tag{2.6}$$

An interesting observation can be made. If, for now, the electric fluctuations are neglected and the transition probability is taken to be a δ-function peaked at the change in $\mathbf{z}$ due to deterministic motion (i.e., $W_\tau = \delta(\Delta\mathbf{z} - \Delta)$), then, taking the limit $\tau \to 0$ in Eq. (2.2) gives

$$\frac{\partial}{\partial t} f(\mathbf{z}, t) + \frac{\partial}{\partial \mathbf{z}} \cdot (\dot{\mathbf{z}} f(\mathbf{z}, t)) = 0, \tag{2.7}$$

which describes the Hamiltonian time evolution of a function $f(\mathbf{z}(t), t)$. This is an expected result, if only Hamiltonian changes in the phase space were allowed, and is in fact exact: the terms of order $\mathcal{O}(\frac{\langle \Delta\Delta \rangle}{\tau})$ and higher vanish as $\tau \to 0$ because in this limit the change in the phase space coordinates approaches $\Delta\mathbf{z} \to \dot{\mathbf{z}}\tau$.

With the electric fluctuations present, the terms of order $\mathcal{O}(\frac{\langle \Delta\Delta\Delta \rangle}{\tau})$ and higher do not vanish completely byt are usually neglected. In plasmas, where the number of particles within the Debye-sphere is large, this approximation is well justified [42]. It can be shown that the first two terms,

$\langle\Delta\rangle$ and $\langle\Delta\Delta\rangle$, include logarithmically divergent terms, eventually leading to a Coulomb logarithm, whereas $\langle\Delta\Delta\Delta\rangle$ and higher order terms do not contain such a divergent term.

The resulting partial differential equation containing both the Hamiltonian motion and collisional effects then is

$$\frac{\partial}{\partial t}f(\mathbf{z},t) = -\frac{\partial}{\partial \mathbf{z}}\cdot\left[(\dot{\mathbf{z}}+\mathbf{a}(\mathbf{z},t))f(\mathbf{z},t)\right] + \frac{\partial}{\partial \mathbf{z}}\frac{\partial}{\partial \mathbf{z}} : \left[\mathbf{D}(\mathbf{z},t)f(\mathbf{z},t)\right], \tag{2.8}$$

and is often referred to as the *kinetic equation* or the kinetic *Fokker-Planck equation*. The collisional friction (or drag) vector and diffusion tensor appearing in the equation, also called the Fokker-Planck coefficients, are defined according to

$$\mathbf{a}(\mathbf{z},t) = \lim_{\tau\to 0}\frac{\langle\Delta\rangle}{\tau}, \tag{2.9}$$

$$\mathbf{D}(\mathbf{z},t) = \lim_{\tau\to 0}\frac{\langle\Delta\Delta\rangle}{2\tau}. \tag{2.10}$$

To emphasize the nature of the collisional contribution, it is customary to write the collisional terms separately from the Hamiltonian contribution, and express the kinetic equation as

$$\frac{\partial}{\partial t}f + \frac{\partial}{\partial \mathbf{z}}\cdot(\dot{\mathbf{z}}f) = C\left[f\right], \tag{2.11}$$

where $C\left[f\right]$ is called the *collision operator* defined as

$$C\left[f\right] = -\frac{\partial}{\partial \mathbf{z}}\cdot\left[\mathbf{a}f - \frac{\partial}{\partial \mathbf{z}}\cdot(\mathbf{D}f)\right] \equiv -\frac{\partial}{\partial \mathbf{z}}\cdot\mathbf{J}, \tag{2.12}$$

and $\mathbf{J}$ is the collisional flux density.

2.2 Correspondence to stochastic differential equations

As the Fokker-Planck coefficients could in principle be arbitrary functions, it is not trivial to find a solution to the kinetic equation. Finite element or finite difference method combined with a time discretization scheme could be considered because the distribution function vanishes at the phase space edge imposing a natural boundary condition. In orbit-averaged studies of collisional transport the phase space contained only three coordinates, and these numerical methods could be suitable. The six dimensions of the full charged particle phase space, however, limit the practicability of the finite elements and other discretization methods.

Fortunately, the origin of the kinetic equation, the random motion of the particles, suggests an intuitive solution: The motion of the particles

should also solve the kinetic equation, as the distribution function essentially is an averaged representation of the particles in the system. Kolmogorov [43, 44] was one of the first to provide a mathematically rigorous connection between evolution of stochastic processes and the Fokker-Planck equation. The result according to Kolmogorov is that if the probability density for a stochastic process $\mathbf{z}$ obeys Eq. (2.8), the time evolution of $\mathbf{z}$ is governed by the stochastic differential equation

$$d\mathbf{z} \;=\; [\dot{\mathbf{z}} + \mathbf{a}(\mathbf{z}, t)]\, dt + \boldsymbol{\sigma} \cdot d\boldsymbol{\beta}, \tag{2.13}$$

where the matrix $\boldsymbol{\sigma}$ is defined via a decomposition of the diffusion tensor

$$2\mathbf{D} = \boldsymbol{\sigma}\boldsymbol{\sigma}^T. \tag{2.14}$$

Here the stochastic differential $d\boldsymbol{\beta}$ denotes an infinitesimal change in the Wiener process $\boldsymbol{\beta}$ which has zero mean and variance t, and the upper index ^{T} denotes a transpose of a matrix. For an introduction to stochastic processes, see, e.g., Ref. [45].

The connection between the kinetic Fokker-Planck equation and the stochastic differential equations is not evident. The connection, however, becomes transparent when the rules of the so-called *Itô calculus* are applied. Assuming that $\mathbf{z}(t)$ is a Itô process, the Itô differential of an arbitrary function $\phi(\mathbf{z})$ of that Itô process is then defined as

$$d\phi = \frac{\partial}{\partial \mathbf{z}}\phi \cdot d\mathbf{z} + \frac{1}{2}\frac{\partial}{\partial \mathbf{z}}\frac{\partial}{\partial \mathbf{z}}\phi : d\mathbf{z}d\mathbf{z}, \tag{2.15}$$

which in ordinary calculus could be be considered as a truncated Taylor expansion of $\phi(\mathbf{z} + d\mathbf{z}) - \phi(\mathbf{z})$. Now, if $\mathbf{z}(t)$ developes in time according to the Eq. (2.13), one can apply the Itô rules for mixed differentials

$$d\mathbf{z}dt = \mathbf{0}, \quad d\boldsymbol{\beta}dt = \mathbf{0}, \quad d\boldsymbol{\beta}d\boldsymbol{\beta} = \boldsymbol{I}dt, \tag{2.16}$$

and obtain

$$d\phi = \frac{\partial}{\partial \mathbf{z}}\phi \cdot [(\dot{\mathbf{z}} + \mathbf{a})dt + \boldsymbol{\sigma} \cdot d\boldsymbol{\beta}] + \frac{\partial}{\partial \mathbf{z}}\frac{\partial}{\partial \mathbf{z}}\phi : \mathbf{D}dt. \tag{2.17}$$

With an initial condition $\mathbf{z}(0) = \mathbf{y}$, one can calculate the value of function $\phi(\mathbf{z})$ at later times according to

$$\begin{aligned}
\phi(\mathbf{z}) =& \phi(\mathbf{y}) + \int_0^t d\phi \\
=& \phi(\mathbf{y}) + \int_0^t \left(\frac{\partial}{\partial \mathbf{z}}\phi \cdot (\dot{\mathbf{z}} + \mathbf{a}) + \frac{\partial}{\partial \mathbf{z}}\frac{\partial}{\partial \mathbf{z}}\phi : \mathbf{D} \right) dt \\
&+ \int_o^t \frac{\partial}{\partial \mathbf{z}}\phi \cdot \boldsymbol{\sigma} \cdot d\boldsymbol{\beta}.
\end{aligned} \tag{2.18}$$

Then, taking the expectation value of Eq. (2.18) with respect to $\mathbf{z}$ gives the Dynkin's formula, a sort of stochastic generalization of the fundamental theorem of calculus,

$$\mathrm{E}^{\mathbf{z}}[\phi(\mathbf{z})] = \phi(\mathbf{y}) + \mathrm{E}^{\mathbf{z}}[\int_0^t A\phi(\mathbf{z})dt], \tag{2.19}$$

where the linear operator A is called the *generator* for the stochastic process $\mathbf{z}(t)$, and is defined as

$$Af(\mathbf{z}) = \frac{\partial}{\partial \mathbf{z}} f \cdot (\dot{\mathbf{z}} + \mathbf{a}) + \frac{\partial}{\partial \mathbf{z}} \frac{\partial}{\partial \mathbf{z}} f : \mathbf{D}. \tag{2.20}$$

In the Dynkin's formula, the contribution from the stochastic term still appearing in Eq. (2.18), vanishes because

$$\mathrm{E}^{\mathbf{z}}[\int_o^t \frac{\partial}{\partial \mathbf{z}} \phi \cdot \boldsymbol{\sigma} \cdot d\boldsymbol{\beta}] = 0. \tag{2.21}$$

The proof can be found for example in Ref. [45].

If $\mathbf{z}$ has a probability density $f(\mathbf{z}, t)$, the expectation value of an arbitrary function of $\mathbf{z}$ can be expressed as

$$\mathrm{E}^{\mathbf{z}}[\phi(\mathbf{z})] = \int \phi(\mathbf{z}) f(\mathbf{z}, t) d\mathbf{z}, \tag{2.22}$$

and the Dynkin's formula becomes

$$\int \phi(\mathbf{z}) f(\mathbf{z}, t) d\mathbf{z} = \phi(\mathbf{y}) + \int \int_0^t A\phi(\mathbf{z}) f(\mathbf{z}, t) dt d\mathbf{z} \tag{2.23}$$

Taking time derivative from both sides gives

$$\begin{aligned} \int \phi(\mathbf{z}) \frac{\partial}{\partial t} f(\mathbf{z}, t) d\mathbf{z} &= \int A\phi(\mathbf{z}) f(\mathbf{z}, t) d\mathbf{z} \\ &= \int \phi(\mathbf{z}) A^\dagger f(\mathbf{z}, t) d\mathbf{z}, \end{aligned} \tag{2.24}$$

where $A^\dagger$ is now the *adjoint* operator of the generator A, and is defined

$$A^\dagger f(\mathbf{z}) = -\frac{\partial}{\partial \mathbf{z}} \cdot [(\dot{\mathbf{z}} + \mathbf{a}) f] + \frac{\partial}{\partial \mathbf{z}} \frac{\partial}{\partial \mathbf{z}} : [\mathbf{D} f]\,. \tag{2.25}$$

Rearranging the terms yields

$$\int \phi(\mathbf{z}) \left(\frac{\partial}{\partial t} f(\mathbf{z}, t) - A^\dagger f(\mathbf{z}, t) \right) d\mathbf{z} = 0, \tag{2.26}$$

and as the function ϕ was arbitrary, it has to be that

$$\frac{\partial}{\partial t} f(\mathbf{z}, t) = A^\dagger f(\mathbf{z}, t) = -\frac{\partial}{\partial \mathbf{z}} \cdot [(\dot{\mathbf{z}} + \mathbf{a}) f] + \frac{\partial}{\partial \mathbf{z}} \frac{\partial}{\partial \mathbf{z}} : [\mathbf{D} f]\,, \tag{2.27}$$

which is the kinetic Fokker-Planck equation derived in the previous section.

2.3 Kinetic theory in particle phase space

Here, the particle motion is formulated in terms of a non-canonical Poisson bracket. This is done as it turns out that the collisional part of the kinetic equation can be expressed with the Poisson bracket. Later, this property will be exploited to conduct a guiding center transformation of the collision operator. Before introducing the guiding center formalism any further, though, the particle phase space Poisson bracket is derived, the collisional Fokker-Planck coefficients for the particle phase space are presented, their conservation properties are discussed, and a stochastic differential equation describing test particle motion is established assuming a Maxwellian background plasma.

2.3.1 Hamiltonian motion

The non-canonical formulation of the charged particle dynamics derives from requiring stationarity for the action path integral

$$\mathcal{A} = \int \gamma, \tag{2.28}$$

with respect to different phase space paths. The differential one-form γ is

$$\gamma = \gamma_\alpha(\boldsymbol{z})\mathrm{d}z^\alpha - H(\boldsymbol{z})\mathrm{d}t, \tag{2.29}$$

where H is the Hamiltonian, and d denotes the *exterior derivative* (see appendix A for the details regarding differential forms and exterior derivative). The one-form γ is, essentially, the differential of the Lagrangian action. The part $\gamma_\alpha \mathrm{d}z^\alpha$ is referred to as the symplectic part and $H\mathrm{d}t$ as the Hamiltonian constraint for the phase space motion. The constraint condition simply states that the particle energy remains constant along the Hamiltonian orbit. For a modern describtion of classical mechanics see, e.g., Ref. [46].

Demanding that the variation of the action integral with respect to different phase space paths $\delta\mathbf{z}$ vanishes, i.e., applying the Hamilton's principle, gives

$$\begin{aligned}
0 &= \delta_{\mathbf{z}} \int \gamma \\
&= \int i_{\delta\mathbf{z}} \cdot \mathrm{d}\gamma \\
&= \int i_{\delta\mathbf{z}} \cdot \left[\frac{1}{2} \left(\frac{\partial \gamma_\beta}{\partial z^\alpha} - \frac{\partial \gamma_\alpha}{\partial z^\beta} \right) \mathrm{d}z^\alpha \wedge \mathrm{d}z^\beta - \frac{\partial H}{\partial z^\alpha} \mathrm{d}z^\alpha \wedge \mathrm{d}t \right] \\
&= \int \delta z^\alpha \left[\omega_{\alpha\beta} \mathrm{d}z^\beta - \frac{\partial H}{\partial z^\alpha} \mathrm{d}t \right],
\end{aligned} \tag{2.30}$$

where $i_{\delta \mathbf{z}}$ is the contraction operator with respect to vector field $\delta \mathbf{z}$ (see the appendix A) and

$$\omega_{\alpha\beta} = \frac{1}{2}\left(\frac{\partial \gamma_\beta}{\partial z^\alpha} - \frac{\partial \gamma_\alpha}{\partial z^\beta}\right), \tag{2.31}$$

is the Lagrange matrix.

As the variation of the path is arbitrary, then, for the integral to vanish, the condition

$$\omega_{\alpha\beta}\frac{dz^\beta}{dt} = \frac{\partial H}{\partial z^\alpha} \tag{2.32}$$

must be true. If the Lagrange matrix is invertible, the equations of motion are then obtained as

$$\frac{dz^\alpha}{dt} = \Pi_{\alpha\beta}\frac{\partial H}{\partial z^\beta} \tag{2.33}$$

where $\Pi_{\alpha\beta}$ is the Poisson matrix satisfying $\omega_{\alpha\beta}\Pi^{\beta\gamma} = \delta^\gamma_\alpha$. Defining the Poisson bracket of two arbitrary functions, f and g, according to

$$\{f, g\} \equiv \frac{\partial f}{\partial z^\alpha}\Pi^{\alpha\beta}\frac{\partial g}{\partial z^\beta}. \tag{2.34}$$

the equations of motion are finally written with the bracket notation as

$$\frac{dz^\alpha}{dt} = \{z^\alpha, H\}. \tag{2.35}$$

The Hamiltonian nature of the equations of motion automatically satisfies the Liouville theorem

$$\frac{\partial}{\partial z^\alpha}\left(\mathcal{J}\frac{dz^\alpha}{dt}\right) = 0, \tag{2.36}$$

stating that the phase space flow is conserved and that the Hamiltonian trajectories never cross. Here $\mathcal{J} = \det \boldsymbol{\omega}$ is the phase space *Jacobian* for the coordinates z^α. The Liouville theorem also gives the Liouville identies

$$\frac{\partial}{\partial z^\alpha}\left(\mathcal{J}\Pi^{\alpha\beta}\right) = 0, \tag{2.37}$$

which imply that the Poisson bracket can be written also in a phase space divergence form

$$\{f, g\} = \frac{1}{\mathcal{J}}\frac{\partial}{\partial z^\alpha}\left(\mathcal{J} f \Pi^{\alpha\beta}\frac{\partial g}{\partial z^\beta}\right). \tag{2.38}$$

To give an example of the non-canonical Hamiltonian formulation, consider the motion of a particle with a charge q and mass m in a magnetic field $\mathbf{B} = \nabla \times \mathbf{A}$. The equations of motion are the familiar duo

$$\dot{\mathbf{v}} = \frac{q}{m}\mathbf{v} \times \mathbf{B}, \tag{2.39}$$

$$\dot{\mathbf{x}} = \mathbf{v}. \tag{2.40}$$

where $\mathbf{z} = (\mathbf{x}, \mathbf{v})$ forms the non-canonical particle phase space. The Hamiltonian is just the kinetic energy

$$H = \frac{1}{2} m v^2, \tag{2.41}$$

and the Lagrangian is given by [47]

$$\begin{aligned} L =& \frac{1}{2} m v^2 + q\mathbf{v} \cdot \mathbf{A} && (2.42)\\ =& (m\mathbf{v} + q\mathbf{A}) \cdot \mathbf{v} - H. && (2.43) \end{aligned}$$

The reason for the term $q\mathbf{v} \cdot \mathbf{A}$ to appear in the Lagrangian is the non-conservative nature of the Lorentz force. The term $\mathbf{v} \times \mathbf{B}$ denotes a force that depends not only on the particles spatial position, but on the velocity as well.

The one-form γ is then defined as

$$\begin{aligned} \gamma =& L \mathrm{d}t && (2.44)\\ =& \ (m\mathbf{v} + q\mathbf{A}) \cdot \mathrm{d}\mathbf{x} - H \mathrm{d}t, && (2.45) \end{aligned}$$

and the 6×6 Lagrange matrix expressed with 3×3 blocks for the $(\mathbf{x}, \mathbf{v})$ phase space becomes

$$\boldsymbol{\omega} = m \begin{pmatrix} \epsilon_{ijk}\Omega^k & -\delta_{ij} \\ \delta_{ij} & \mathbf{0} \end{pmatrix}, \tag{2.46}$$

where $\Omega^k = qB^k/m$, and $i, j, k \in \{1, 2, 3\}$. Inversion of the Lagrange matrix gives the Poisson matrix

$$\boldsymbol{\Pi} = m^{-1} \begin{pmatrix} \mathbf{0} & \delta^{ij} \\ -\delta^{ij} & \epsilon^{ijk}\Omega_k \end{pmatrix}, \tag{2.47}$$

and the Poisson bracket can be written explicitly as

$$\{f, g\} = \frac{1}{m} \left(\nabla f \cdot \frac{\partial g}{\partial \mathbf{v}} - \frac{\partial f}{\partial \mathbf{v}} \cdot \nabla g \right) + \frac{q\mathbf{B}}{m^2} \cdot \frac{\partial f}{\partial \mathbf{v}} \times \frac{\partial g}{\partial \mathbf{v}}. \tag{2.48}$$

With the bracket and the Hamiltion it is then easy to confirm that the Lagrangian approach yields the very same equations of motion it was supposed to.

As a last note, it is pointed out that the Poisson-bracket can be used to express the momentum gradient of an arbitrary function as

$$\frac{\partial f}{\partial \mathbf{p}} = \{\mathbf{x}, f\}. \tag{2.49}$$

Later, this property is used to conduct the guiding center transformation of the Coulomb collision operator.

2.3.2 Coulomb collisions

The Coulomb collisions change the particles velocity coordinates as illustrated in Fig. 2.1, and can be considered as instantaneous jumps from one Hamiltonian orbit to another, as discussed earlier. Thus, the collision operator in Eq. (2.12) acts only in the velocity space and becomes

$$C[f] = -\frac{\partial}{\partial \mathbf{v}} \cdot \left[\mathbf{a} f - \frac{\partial}{\partial \mathbf{v}} \cdot (\mathbf{D} f) \right]. \tag{2.50}$$

The explicit expressions for the Coulomb friction and diffusion coefficients describing the collisions of species a with other plasma particles are

$$\mathbf{a}_a = -\sum_b \frac{c_{ab}}{m_a^2} \left(1 + \frac{m_a}{m_b}\right) \int d\mathbf{v}' f_b(\mathbf{v}') \frac{\mathbf{u}}{u^3} = \sum_b \mathbf{a}_{ab} \tag{2.51}$$

$$\mathbf{D}_a = \frac{1}{2} \sum_b \frac{c_{ab}}{m_a^2} \int d\mathbf{v}' f_b(\mathbf{v}') \left(\frac{\mathbf{I}}{u} - \frac{\mathbf{uu}}{u^3} \right) = \sum_b \mathbf{D}_{ab}, \tag{2.52}$$

where $c_{ab} = q_a^2 q_b^2 \ln\Lambda/\epsilon_0$, $\ln\Lambda$ is the Coulomb logarithm, q_b and f_b are the electric charge and the distribution function of the plasma species b respectively, and $\mathbf{u} = \mathbf{v} - \mathbf{v}'$. For a comprehensive derivation of the coefficients, see Refs. [42, 48].

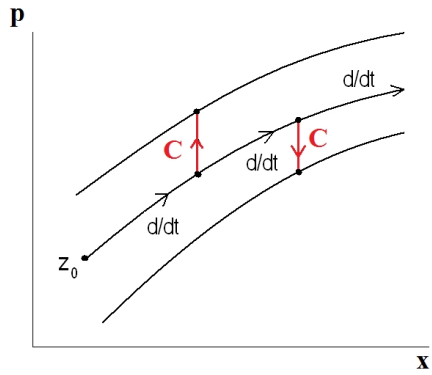

Figure 2.1. A Schematic view of Coulomb collision changing the phase space coordinates of a particle. the time derivative refers to the Hamiltonian motion and the red C to a Coulomb collision. Courtesy of Alain Brizard.

The friction and diffusion coefficients can be expressed also as

$$\mathbf{a}_{ab} = \frac{c_{ab}}{m_a^2} \left(1 + \frac{m_a}{m_b}\right) \frac{\partial h_b}{\partial \mathbf{v}}, \tag{2.53}$$

$$\mathbf{D}_{ab} = \frac{1}{2} \frac{c_{ab}}{m_a^2} \frac{\partial}{\partial \mathbf{v}} \frac{\partial}{\partial \mathbf{v}} g_b, \tag{2.54}$$

where the *Rosenbluth* or *Trubnikov potentials*, h_b and g_b, are defined

$$h_b(\mathbf{v}) = \int d\mathbf{v}' f_b(\mathbf{v}') \frac{1}{|\mathbf{v}-\mathbf{v}'|}, \tag{2.55}$$

$$g_b(\mathbf{v}) = \int d\mathbf{v}' f_b(\mathbf{v}') \left|\mathbf{v}-\mathbf{v}'\right|. \tag{2.56}$$

As the potentials (referring to electrostatic analogy) satisfy the Poisson equation

$$\frac{\partial}{\partial \mathbf{v}} \cdot \frac{\partial}{\partial \mathbf{v}} g_b = 2h_b, \tag{2.57}$$

one can identify a useful relation between the Fokker-Planck coefficients

$$\mathbf{a}_{ab} = \left(1 + \frac{m_a}{m_b}\right) \frac{\partial}{\partial \mathbf{v}} \cdot \mathbf{D}_{ab}, \tag{2.58}$$

and use it to transform the collision operator into the *Landau form*

$$C_{ab}\left[f_a\right] = \frac{\partial}{\partial \mathbf{v}} \cdot \frac{1}{2}\frac{c_{ab}}{m_a} \int d\mathbf{v}' \left(\frac{\mathbf{I}}{u} - \frac{\mathbf{uu}}{u^3}\right) \cdot \left(\frac{f_b(\mathbf{v}')}{m_a}\frac{\partial f_a}{\partial \mathbf{v}} - \frac{f_a(\mathbf{v})}{m_b}\frac{\partial f_b}{\partial \mathbf{v}'}\right), \tag{2.59}$$

or, alternatively, into a form

$$C_{ab}\left[f_a\right] = -\frac{\partial}{\partial \mathbf{v}} \cdot \left(\mathbf{K}_{ab} f_a - \mathbf{D}_{ab} \cdot \frac{\partial f_a}{\partial \mathbf{v}}\right), \tag{2.60}$$

where

$$\mathbf{K}_{ab} = \frac{m_a}{m_b}\frac{\partial}{\partial \mathbf{v}} \cdot \mathbf{D}_{ab} = \frac{c_{ab}}{m_a^2}\frac{m_a}{m_b}\frac{\partial}{\partial \mathbf{v}} h_b. \tag{2.61}$$

The latter form proves itself useful regearding the guiding center transformation of the collision operator. It is possible to express the particle collision operator in terms of the non-canonical Poisson bracket as

$$C_{ab}\left[f\right] = \{x^i, m_a K^i_{ab} f_a - m_a^2 D^{ij}_{ab}\{x^j, f_a\}\}, \tag{2.62}$$

and obtain the guiding center collision operator by transforming the particle Poisson bracket into guiding center Poisson bracket (see Chapter. 3).

With the Landau form one demonstrates the conservation properties of the collision operator. As the operator is expressed as a divergence of the collisional flux density, the collisional part of the kinetic equation takes the form of a conservation law. Thus, it automatically preserves the particle number. Regarding the momentum conservation, the Landau form is used to calculate the momentum transfer rate between species a and b according to

$$\begin{aligned} \dot{\mathbf{p}}_{ab} &= \int \mathrm{d}\mathbf{v}\; m_a \mathbf{v}\; C_{ab}\left[f\right], \\ &= -\frac{1}{2} c_{ab} \int d\mathbf{v} \int d\mathbf{v}' \left(\frac{\mathbf{I}}{u} - \frac{\mathbf{uu}}{u^3}\right) \cdot \left(\frac{f_b(\mathbf{v}')}{m_a}\frac{\partial f_a}{\partial \mathbf{v}} - \frac{f_a(\mathbf{v})}{m_b}\frac{\partial f_b}{\partial \mathbf{v}'}\right). \end{aligned} \tag{2.63}$$

As the momentum transfer rate is inherently antisymmetric with respect to the species, the momentum conservation is proved upon making the replacement $a \leftrightarrow b$, and observing that $\dot{\mathbf{p}}_{ab} = -\dot{\mathbf{p}}_{ba}$. One also verifies that $\dot{\mathbf{p}}_{aa} = 0$, i.e., that the total momentum of species a is conserved in like-species collisions.

For the energy transfer rate a similar calculation gives

$$\dot{E}_{ab} = -\frac{1}{4} c_{ab} \int d\mathbf{v} \int d\mathbf{v}' \; \mathbf{v} \cdot \left(\frac{\mathbf{I}}{u} - \frac{\mathbf{u}\mathbf{u}}{u^3} \right) \cdot \left(\frac{f_b(\mathbf{v}')}{m_a} \frac{\partial f_a}{\partial \mathbf{v}} - \frac{f_a(\mathbf{v})}{m_b} \frac{\partial f_b}{\partial \mathbf{v}'} \right), \quad (2.64)$$

which no longer is antisymmetric because of the extra $\mathbf{v}$ inside the integrals. Upon making the replacements $a \leftrightarrow b$ and $\mathbf{v} \leftrightarrow \mathbf{v}'$ one obtains

$$\dot{E}_{ba} = \frac{1}{4} c_{ab} \int d\mathbf{v} \int d\mathbf{v}' \; \mathbf{v}' \cdot \left(\frac{\mathbf{I}}{u} - \frac{\mathbf{u}\mathbf{u}}{u^3} \right) \cdot \left(\frac{f_b(\mathbf{v}')}{m_a} \frac{\partial f_a}{\partial \mathbf{v}} - \frac{f_a(\mathbf{v})}{m_b} \frac{\partial f_b}{\partial \mathbf{v}'} \right), \quad (2.65)$$

and adding Eqs. (2.64) and (2.65) together gives $\dot{E}_{ab} + \dot{E}_{ba} = 0$ because

$$(\mathbf{v} - \mathbf{v}') \cdot \left(\frac{\mathbf{I}}{u} - \frac{\mathbf{u}\mathbf{u}}{u^3} \right) = \mathbf{0}. \quad (2.66)$$

Thus the collision operator conserves the energy, and $\dot{E}_{aa} = 0$ holds.

2.3.3 Stochastic differential equation for a charged particle

If the bulk of the plasma, i.e., the field particles, form isotropic distributions, the Rosenbluth potentials, $h_b(\mathbf{v}) = h_b(\mathrm{v})$ and $g_b(\mathbf{v}) = g_b(\mathrm{v})$, become functions of particle energy only. The friction and diffusion coefficients can then be simplified into

$$\mathbf{a}_{ab} = -\left(1 + \frac{m_b}{m_a}\right) \nu_{ab} \, \mathbf{v}, \quad (2.67)$$

$$\mathbf{K}_{ab} = -\nu_{ab} \, \mathbf{v}, \quad (2.68)$$

$$\mathbf{D}_{ab} = D_{\parallel,ab} \frac{\mathbf{v}\mathbf{v}}{v^2} + D_{\perp,ab} \left(\mathbf{I} - \frac{\mathbf{v}\mathbf{v}}{v^2} \right), \quad (2.69)$$

where the scalar coefficients are defined

$$\nu_{ab} = -\frac{c_{ab}}{m_a^2} \frac{m_a}{m_b} \frac{1}{v} h_b'(v), \quad (2.70)$$

$$D_{\parallel,ab} = \frac{1}{2} \frac{c_{ab}}{m_a^2} g_b''(v), \quad (2.71)$$

$$D_{\perp,ab} = \frac{1}{2} \frac{c_{ab}}{m_a^2} \frac{1}{v} g_b'(v). \quad (2.72)$$

Then, observing the identities

$$\left(\mathbf{I} - \frac{\mathbf{v}\mathbf{v}}{v^2} \right) \cdot \left(\mathbf{I} - \frac{\mathbf{v}\mathbf{v}}{v^2} \right) = \left(\mathbf{I} - \frac{\mathbf{v}\mathbf{v}}{v^2} \right), \quad (2.73)$$

$$\frac{\mathbf{v}\mathbf{v}}{v^2} \cdot \left(\mathbf{I} - \frac{\mathbf{v}\mathbf{v}}{v^2} \right) = \mathbf{0}, \quad (2.74)$$

$$\frac{\mathbf{v}\mathbf{v}}{v^2} \cdot \frac{\mathbf{v}\mathbf{v}}{v^2} = \frac{\mathbf{v}\mathbf{v}}{v^2}, \quad (2.75)$$

the decomposition of the diffusion matrix according to Eq. (2.14) becomes rather simple:

$$\boldsymbol{\sigma} = \sqrt{2D_\parallel}\frac{\mathbf{vv}}{v^2} + \sqrt{2D_\perp}\left(\mathbf{I} - \frac{\mathbf{vv}}{v^2}\right), \tag{2.76}$$

where $D_\parallel = \sum_b D_{\parallel,ab}$ and $D_\perp = \sum_b D_{\perp,ab}$. By direct calculation, one can verify that $\boldsymbol{\sigma}\boldsymbol{\sigma}^T = 2\mathbf{D}$.

The stochastic differential equation describing the particle motion is constructed according to Eq. (2.13). As the Coulomb collisions only affect the particles velocity coordinates, the equation for the spatial position reduces to the Hamiltonian motion:

$$d\mathbf{x} = \mathbf{v}dt. \tag{2.77}$$

For the velocity, the equation includes also the Coulomb drag and diffusion, and is explicitly

$$d\mathbf{v} = \left(\frac{q}{m}\mathbf{v}\times\mathbf{B} - \nu_s\mathbf{v}\right)dt + \left(\sqrt{2D_\parallel}\frac{\mathbf{vv}}{v^2} + \sqrt{2D_\perp}\left(\mathbf{I} - \frac{\mathbf{vv}}{v^2}\right)\right)\cdot d\boldsymbol{\beta}^{\mathbf{v}}, \tag{2.78}$$

where $\nu_s = \sum_b (1 + m_b/m_a)\nu_{ab}$.

An important case of isotropic particle distributions is the Maxwellian distribution. In minority particle studies, the field particle distributions are often approximated to be in thermodynamic equilibrium and, thus, roughly Maxwellian:

$$f_b = \frac{n_b}{\pi^{3/2}v_b^3}\exp\left(-v^2/v_b^2\right), \tag{2.79}$$

where $v_b = \sqrt{2kT_b/m_b}$ and n_b are, respectively, the thermal velocity and density of the field particle species b. With this assumption, explicit expressions for the scalar friction and diffusion coefficients can be calculated. The Rosenbluth potentials become

$$h_b = \frac{n_b}{v}\mathrm{erf}(v/v_b), \tag{2.80}$$

$$g_b = n_b v_b \varphi(v/v_b), \tag{2.81}$$

where $\mathrm{erf}(x) = 2\pi^{-1/2}\int_0^x dt\exp(-t^2)$ is the *Error function*, and $\varphi(x) = (x + 1/(2x))\mathrm{erf}(x) + \pi^{-1/2}\exp(-x^2)$. Thus, the scalar coefficients can be given specific expressions

$$D_{\parallel,ab}(v) = \frac{1}{2}\frac{c_{ab}}{m_a^2}\frac{n_b}{v}G(v/v_b), \tag{2.82}$$

$$D_{\perp,ab}(v) = \frac{1}{2}\frac{c_{ab}}{m_a^2}\frac{n_b}{v}\left(\mathrm{erf}(v/v_b) - \frac{1}{2}G(v/v_b)\right), \tag{2.83}$$

$$\nu_{ab}(v) = \frac{c_{ab}}{m_a^2}\frac{m_a}{m_b}\frac{n_b}{v_b^2}\frac{G(v/v_b)}{v}. \tag{2.84}$$

where the Chandrasekhar function $G(x)$ is defined as

$$G(x) = \frac{\mathrm{erf}(x) - \frac{2x}{\sqrt{\pi}} \exp(-x^2)}{x^2}. \tag{2.85}$$

With the coefficients in the kinetic equation specified and a stochastic differential equation explicitly given, the kinetic equation can be solved via numerical simulation. The Hamiltonian particle motion, however, is characterized by the rapid cyclotron motion, which sets a strict limit for the length of the simulation time step, and compromises the practicability of using the particle phase space in numerical transport studies. Fortunately, the particle kinetic equation can be used as a starting point for constructing the guiding center kinetic equation, where the rapid time scale is no longer present but is isolated into non-contributing variables.

3. Guiding center formalism

The aim of this chapter is to provide a description of collisional transport in terms of a reduced phase space where the rapid gyromotion is irrelevant for both the Hamiltonian motion and Coulomb collisions. For this task, *Lie-transform perturbation methods* are applied to the particle kinetic equation and the modern guiding center theory is obtained. The description of Hamiltonian guiding center motion presented here follows previous derivations [31, 32], intending to elaborate the process more explicitly. The derivation of the guiding center kinetic equation is then carried out according to the work of Brizard [40], providing an example of how the guiding center friction and diffusion coefficients are calculated. Finally, an important proof missing from Publication III is explicitly given to show that the guiding center diffusion matrix is positive semidefinite and that the stochastic differential equation describing both the Hamiltonian and collisional motion of the guiding center can be constructed also in nonunifrom magnetic field.

3.1 Preparations for the guiding center transformation

The local particle coordinates, $z^\alpha = (\mathbf{x}_0, \mathbf{v}_0)$, are first written as $z^\alpha = (\mathbf{x}_0, v_{\parallel,0}, \mu_0, \zeta_0)$, where $v_{\parallel,0}$ is the particle velocity parallel to the magnetic field, μ_0 is the particles local magnetic moment, and ζ_0 is the gyroangle describing the rapid rotation around the magnetic axis. Then, a set of local rotating orthonormal basis vectors, $(\widehat{\mathbf{b}}(\mathbf{x}_0), \widehat{\perp}(\zeta_0, \mathbf{x}_0), \widehat{\boldsymbol{\rho}}(\zeta_0, \mathbf{x}_0))$, with $\boldsymbol{\rho} = \mathbf{b} \times \mathbf{v}/\Omega$ and $\Omega = qB/m$, is introduced to express the particle velocity with components parallel and perpendicular to the magnetic field

$$\mathbf{v} = v_{\parallel,0}\widehat{\mathbf{b}} + \sqrt{\frac{2\mu_0 B}{m}}\widehat{\perp} = v_{\parallel,0}\widehat{\mathbf{b}} + \Omega\boldsymbol{\rho} \times \widehat{\mathbf{b}} = v_{\parallel,0}\widehat{\mathbf{b}} + \mathbf{v}_{0,\perp}. \tag{3.1}$$

The rotating basis is determined with another basis, $(\widehat{\mathbf{1}}(\mathrm{x}_0), \widehat{\mathbf{2}}(\mathrm{x}_0))$, according to

$$\widehat{\boldsymbol{\rho}} = \cos\zeta_0\widehat{\mathbf{1}} - \sin\zeta_0\widehat{\mathbf{2}}, \tag{3.2}$$

$$\widehat{\perp} = -\sin\zeta_0\widehat{\mathbf{1}} - \cos\zeta_0\widehat{\mathbf{2}}, \tag{3.3}$$

and one could wonder what the definition for the fixed basis $(\widehat{\mathbf{1}}, \widehat{\mathbf{2}})$ is but, later, it is proven that the choice is free and does not affect the resulting guiding center motion.

A small parameter, $\epsilon_B = \rho/L_B$, where $L_B = B/|\nabla B|$ is the local magnetic field gradient length, is used to rate the terms in the particle Lagrangian one-form for initial ordering. As $\epsilon_B \sim m/q$, and the symplectic part of the particle one-form contains this ratio, a dimensionless ordering parameter ϵ, which is not to be mixed with ϵ_B, can be introduced by renormalization of the particle charge, $q \to \epsilon^{-1}q$. The symplectic part of the particle one-form then is

$$\gamma_\alpha \mathrm{d}z^\alpha = \epsilon^{-1}q\mathbf{A}\cdot\mathrm{d}\mathbf{x} + m\mathbf{v}\cdot\mathrm{d}\mathbf{x} = \epsilon^{-1}\gamma_0 + \gamma_1. \tag{3.4}$$

One should note that ϵ is only the ordering parameter, and physical results are obtained setting $\epsilon = 1$.

The Lie-transform *pull-back* and *push-forward* operators are defined as

$$\mathcal{T}_n = \exp(\epsilon^n \mathcal{L}_{\boldsymbol{G}_n}), \tag{3.5}$$

$$\mathcal{T}_n^{-1} = \exp(-\epsilon^n \mathcal{L}_{\boldsymbol{G}_n}), \tag{3.6}$$

where $\mathcal{L}_{\boldsymbol{G}_n}$ is the *Lie-derivative* generated by a vector field $\boldsymbol{G}_n$, and ϵ^n is used to denote the order of the transformation, when necessary. The Lie-derivative of a k-form γ is defined

$$\mathcal{L}_{\boldsymbol{G}}\gamma = i_{\boldsymbol{G}}\cdot\mathrm{d}\gamma + \mathrm{d}\left(i_{\boldsymbol{G}}\cdot\gamma\right), \tag{3.7}$$

where $i_{\boldsymbol{G}}$ is the contraction operator and d the exterior derivative.

An example of a Lie-transformation can be given if $\boldsymbol{G} = a$ is a constant and the transformation is applied to a scalar function $f(x)$ and to its argument x giving

$$\exp(\mathcal{L}_{\boldsymbol{G}})x = x + a, \tag{3.8}$$

$$\exp(\mathcal{L}_{\boldsymbol{G}})f(x) = f(x + a). \tag{3.9}$$

Referring to $\mathcal{T}$ as a transformation is then well justified, as the operation generated by the field $\boldsymbol{G}$ is a coordinate transformation $x \to X = x + a$.

The Lie-transformation also has an important property, called the the scalar invariance: the transformations defined with (3.5) and (3.6) satisfy

$$(\mathcal{T}_n^{-1} f)(\mathcal{T}_n x) = f(x). \tag{3.10}$$

This property is easily demonstrated if the generating vector field is a constant a: $(\mathcal{T}^{-1} f)(\mathcal{T} x) = f(\mathcal{T} x - a) = f(x + a - a) = f(x)$.

The ultimate goal of the perturbation theory is then to generate the near-identity coordinate transformations, $\mathcal{T}_{gc} : z^\alpha \to Z^\alpha$ and $\mathcal{T}_{gc}^{-1} : Z^\alpha \to z^\alpha$, where $Z^\alpha = (\mathbf{X}, v_\parallel, \mu, \zeta)$ are the guiding center coordinates, and $\mathcal{T}_{gc} = \mathcal{T}_1 \mathcal{T}_2 \mathcal{T}_3 ...$ and $\mathcal{T}_{gc}^{-1} = \ ...\mathcal{T}_3^{-1} \mathcal{T}_2^{-1} \mathcal{T}_1^{-1}$ are the guiding center pull-back and push-forward operators, respectively. The generating functions for the guiding center transformation are free parameters and are solved from the condition that the transformed particle Lagrangian one-form and, thus, also the Hamiltonian motion, become independent of the fast gyro-angle, ζ, order by order.

3.2 Lie-transform perturbation theory

According to the definitions of the Lie-transformations, the guiding center pull-back, $\mathcal{T}_{gc}$, and push-forward $\mathcal{T}_{gc}^{-1}$ are

$$\mathcal{T}_{gc} = 1 + \epsilon \mathcal{L}_{\boldsymbol{G}_1} + \epsilon^2 \left(\mathcal{L}_{\boldsymbol{G}_2} + \frac{1}{2} \mathcal{L}_{\boldsymbol{G}_1}^2 \right) + ..., \tag{3.11}$$

$$\mathcal{T}_{gc}^{-1} = 1 - \epsilon \mathcal{L}_{\boldsymbol{G}_1} - \epsilon^2 \left(\mathcal{L}_{\boldsymbol{G}_2} - \frac{1}{2} \mathcal{L}_{\boldsymbol{G}_1}^2 \right) + ... \tag{3.12}$$

and the guiding center transformation of the symplectic part of the particle one-form is

$$\Gamma = \mathcal{T}_{gc}^{-1} \left(\epsilon^{-1} \gamma_0 + \gamma_1 \right) + \mathrm{d}S = \epsilon^{-1} \Gamma_0 + \Gamma_1 + \epsilon \Gamma_2 + ..., \tag{3.13}$$

where the first three terms in the serie are

$$\Gamma_0 = \gamma_0, \tag{3.14}$$

$$\Gamma_1 = \gamma_1 - \mathcal{L}_{\boldsymbol{G}_1} \gamma_0 + \mathrm{d}S_1, \tag{3.15}$$

$$\Gamma_2 = -\left(\mathcal{L}_{\boldsymbol{G}_2} - \frac{1}{2} \mathcal{L}_{\boldsymbol{G}_1}^2 \right) \gamma_0 - \mathcal{L}_{\boldsymbol{G}_1} \gamma_1 + \mathrm{d}S_2. \tag{3.16}$$

and the terms are evaluated in the guiding center phase space Z^α. The gauge functions S_n are included for a possibility to clean up terms like $\mathrm{d}\left(i_{\boldsymbol{G}_n} \cdot \gamma\right)$ which arise when Lie-derivative is applied. The gauge functions S_n, however, do not contribute to the resulting Lagrangian matrix in any order, nor to the equations of motion, because $\boldsymbol{\omega} = \mathrm{d}\Gamma + \mathrm{d}^2 S = \mathrm{d}\Gamma$.

The explicit expression for the first term in the guiding center Lagrangian one-form Γ is simply

$$\Gamma_0 = q\mathbf{A}(\mathbf{X}) \cdot \mathrm{d}\mathbf{X}, \tag{3.17}$$

but for the second term, Γ_1, the calculation rule of Lie-derivative, given in Eq. (3.7), has to be applied. Direct calculation then reveals that

$$\mathcal{L}_{\boldsymbol{G}_n}\gamma_0 = q\mathbf{B} \times \boldsymbol{G}_n^{\mathbf{X}} \cdot \mathrm{d}\mathbf{X} + \mathrm{d}\left(i_{\boldsymbol{G}_n} \cdot \gamma_0\right), \tag{3.18}$$

and one can write the first order perturbative term as

$$\Gamma_1 = mv_\parallel \widehat{\mathbf{b}} \cdot \mathrm{d}\mathbf{X} + m\Omega \left(\boldsymbol{\rho}_0 \times \widehat{\mathbf{b}} - \widehat{\mathbf{b}} \times \boldsymbol{G}_1^{\mathbf{X}}\right) \cdot \mathrm{d}\mathbf{X} + \mathrm{d}\sigma_1, \tag{3.19}$$

where $\boldsymbol{\rho}_0 = \frac{m}{q}\sqrt{\frac{2\mu_0}{mB}}\widehat{\boldsymbol{\rho}}$ and $\sigma_1 = S_1 - i_{\boldsymbol{G}_1} \cdot \gamma_0$. Thus, choosing the $\mathbf{X}$-component of the first generating vector field to be

$$\boldsymbol{G}_1^{\mathbf{X}} = -\boldsymbol{\rho}_0 + G_{1,\parallel}^{\mathbf{X}} \widehat{\mathbf{b}}, \tag{3.20}$$

the gyro-angle dependency is removed from the first order term of the guiding center Lagrangian one-form. Furthermore, choosing the gauge function $S_1 = i_{\boldsymbol{G}_1} \cdot \gamma_0$ makes σ_1 disappear and one concludes that

$$\Gamma_1 = mv_\parallel \widehat{\mathbf{b}} \cdot \mathrm{d}\mathbf{X}. \tag{3.21}$$

Even though the elimination was successful, it did not specify the generating vector field completely. More components are obtained investigating the second order term, Γ_2, which, after applying the Lie-derivatives, gives

$$\Gamma_2 = -\, i_{\boldsymbol{G}_2} \cdot \mathrm{d}\gamma_0 - \frac{1}{2} i_{\boldsymbol{G}_1} \cdot \mathrm{d}\left(\gamma_1 + \Gamma_1\right) + \mathrm{d}\sigma_2, \tag{3.22}$$

with $\sigma_2 = S_2 - i_{\boldsymbol{G}_1} \cdot \gamma_1$. Using the expression for Γ_1, that was just obtained in Eq. (3.21), the contractions with respect to vector field $\boldsymbol{G}_n$ needed for Γ_2 are

$$i_{\boldsymbol{G}_n} \cdot \mathrm{d}\Gamma_1 = m\widehat{\mathbf{b}} \cdot \left(G_n^{v_\parallel} \mathrm{d}\mathbf{X} - \boldsymbol{G}_n^{\mathbf{X}} \mathrm{d}v_\parallel\right) - mv_\parallel \boldsymbol{G}^{\mathbf{X}} \times \nabla \times \widehat{\mathbf{b}} \cdot \mathrm{d}\mathbf{X}, \tag{3.23}$$

$$\begin{aligned} i_{\boldsymbol{G}_n} \cdot \mathrm{d}\gamma_1 =& i_{\boldsymbol{G}_n} \cdot \mathrm{d}\Gamma_1 - m\boldsymbol{G}^{\mathbf{X}} \times \nabla \times \mathbf{v}_\perp \cdot \mathrm{d}\mathbf{X} \\ &+ m\frac{\partial \mathbf{v}_\perp}{\partial \mu} \cdot \left(G_n^\mu \mathrm{d}\mathbf{X} - \boldsymbol{G}_n^{\mathbf{X}} \mathrm{d}\mu\right) + m\frac{\partial \mathbf{v}_\perp}{\partial \zeta} \cdot \left(G_n^\zeta \mathrm{d}\mathbf{X} - \boldsymbol{G}_n^{\mathbf{X}} \mathrm{d}\zeta\right). \end{aligned} \tag{3.24}$$

Applying the identity given by Eq. (3.18), the expression for Γ_2 becomes

$$\begin{aligned} \Gamma_2 =& -\mathrm{d}\mathbf{X} \cdot \left(q\mathbf{B} \times \boldsymbol{G}_2^{\mathbf{X}} + m\widehat{\mathbf{b}} G_1^{v_\parallel} + \frac{m}{2}\frac{\partial \mathbf{v}_\perp}{\partial \mu} G_1^\mu + \frac{m}{2}\frac{\partial \mathbf{v}_\perp}{\partial \zeta} G_1^\zeta\right) \\ &- \mathrm{d}\mathbf{X} \cdot \left(mv_\parallel \nabla \times \widehat{\mathbf{b}} + \frac{m}{2}\nabla \times \mathbf{v}_\perp\right) \times \boldsymbol{G}_1^{\mathbf{X}} \\ &+ mG_{1,\parallel}^{\mathbf{X}} \mathrm{d}v_\parallel + \frac{m\mu}{q}\mathrm{d}\zeta + \mathrm{d}\sigma_2, \end{aligned} \tag{3.25}$$

where also the results

$$\frac{\partial \mathbf{v}_\perp}{\partial \mu} = \frac{v_\perp}{2\mu}\widehat{\boldsymbol{\rho}} \times \widehat{\mathbf{b}} \quad \Rightarrow \quad \frac{\partial \mathbf{v}_\perp}{\partial \mu} \cdot \boldsymbol{G}_1^{\mathbf{X}} = 0, \tag{3.26}$$

$$\frac{\partial \mathbf{v}_\perp}{\partial \zeta} = -v_\perp \widehat{\boldsymbol{\rho}} \quad \Rightarrow \quad \frac{\partial \mathbf{v}_\perp}{\partial \zeta} \cdot \boldsymbol{G}_1^{\mathbf{X}} = \frac{2\mu}{q}, \tag{3.27}$$

were needed to obtain the final form.

But now, a serious problem is faced because of the term $(m\mu/q)\mathrm{d}\zeta$ appearing in Γ_2. For the Hamiltonian dynamics to be free of both ζ and the way the gyro-angle is defined, the guiding center one-form should remain invariant under a redefinition

$$\zeta \to \zeta' = \zeta + \chi(\mathbf{X}), \tag{3.28}$$

and its components should be independent of ζ. The latter condition is obtained by a careful choice of the generating functions, but the term $(m\mu/q)\mathrm{d}\zeta$ in Γ_2 does not remain invariant under such a transformation. Instead, a term, $(m\mu/q)\nabla\chi \cdot \mathrm{d}\mathbf{X}$, would appear.

To keep Γ_2 invariant, a gyrogauge invariance constraint is needed, and $\mathrm{d}\zeta$ is replaced with $\mathrm{d}\zeta - \boldsymbol{R} \cdot \mathrm{d}\mathbf{X}$, where $\boldsymbol{R}$ is called the gyrogauge field. Then, for the constrained one-form to be independent of the definition of ζ, the condition

$$\begin{aligned} \mathrm{d}\zeta - \boldsymbol{R} \cdot \mathrm{d}\mathbf{X} &= \mathrm{d}\zeta' - \boldsymbol{R}' \cdot \mathrm{d}\mathbf{X} \\ &= \mathrm{d}\zeta + \nabla\chi \cdot \mathrm{d}\mathbf{X} - \boldsymbol{R}' \cdot \mathrm{d}\mathbf{X}, \end{aligned} \tag{3.29}$$

must hold, which further implies that $\boldsymbol{R}$ must satisfy

$$\boldsymbol{R}' = \boldsymbol{R} + \nabla\chi. \tag{3.30}$$

Littlejohn has proved that the choice $\boldsymbol{R} = \nabla\widehat{\mathbf{1}} \cdot \widehat{\mathbf{2}} = \nabla\widehat{\perp} \cdot \widehat{\boldsymbol{\rho}}$ fulfills the criterion [31], and that the guiding center theory can be made independent of the definition of the gyroangle.

As the gyrogauge invariance is assured, the second order term can be further simplified by specifying more components for the generating field. Calculating first

$$\nabla \times \widehat{\mathbf{b}} \times \boldsymbol{G}_1^{\mathbf{X}} = G_{1,\parallel}^{\mathbf{X}}\boldsymbol{\kappa} + \tau\frac{\partial \boldsymbol{\rho}_0}{\partial \zeta} + \boldsymbol{\rho}_0 \cdot \boldsymbol{\kappa}\widehat{\mathbf{b}}, \tag{3.31}$$

where $\boldsymbol{\kappa} = \widehat{\mathbf{b}} \cdot \nabla\widehat{\mathbf{b}}$ and $\tau = \widehat{\mathbf{b}} \cdot \nabla \times \widehat{\mathbf{b}}$, and then

$$\begin{aligned} \nabla \times \mathbf{v}_\perp \times \boldsymbol{G}_1^{\mathbf{X}} = \frac{2\mu}{q}\left(\boldsymbol{R} + \frac{1}{2}\tau\widehat{\mathbf{b}} - (\mathbf{a}_1 : \nabla\widehat{\mathbf{b}} + \tau)\widehat{\mathbf{b}}\right) \\ - \mu\boldsymbol{\rho}_0 \cdot \nabla \ln B\frac{\partial \mathbf{v}_\perp}{\partial \mu} \\ + G_{1,\parallel}^{\mathbf{X}}\left(\nabla \times \mathbf{v}_\perp\right) \times \widehat{\mathbf{b}} + \boldsymbol{\rho}_0 \cdot \boldsymbol{R}\frac{\partial \mathbf{v}_\perp}{\partial \zeta}, \end{aligned} \tag{3.32}$$

where $\mathbf{a}_1 = -(\widehat{\perp}\widehat{\boldsymbol{\rho}} + \widehat{\boldsymbol{\rho}}\widehat{\perp})/2$, the second order term Γ_2 can be given an expression

$$\begin{aligned}\Gamma_2 =& -\mathrm{d}\mathbf{X}\cdot\left(q\mathbf{B}\times\boldsymbol{G}_2^{\mathbf{X}} + mv_\parallel\tau\frac{\partial\boldsymbol{\rho}_0}{\partial\zeta}\right)\\ &-\left(\mathrm{d}\mathbf{X}\cdot\left[mv_\parallel\boldsymbol{\kappa}+\frac{m}{2}\nabla\times\mathbf{v}_\perp\times\widehat{\mathbf{b}}\right]-m\mathrm{d}v_\parallel\right)G_{1,\parallel}^{\mathbf{X}}\\ &-\mathrm{d}\mathbf{X}\cdot m\widehat{\mathbf{b}}\left(G_1^{v_\parallel}+v_\parallel\boldsymbol{\rho}_0\cdot\boldsymbol{\kappa}-\frac{\mu}{q}(\mathbf{a}_1:\nabla\widehat{\mathbf{b}}+\tau)\right)\\ &-\mathrm{d}\mathbf{X}\cdot\frac{m}{2}\frac{\partial\mathbf{v}_\perp}{\partial\mu}\left(G_1^{\mu}-\mu\boldsymbol{\rho}_0\cdot\nabla\ln B\right)\\ &-\mathrm{d}\mathbf{X}\cdot\frac{m}{2}\frac{\partial\mathbf{v}_\perp}{\partial\zeta}\left(G_1^{\zeta}+\boldsymbol{\rho}_0\cdot\boldsymbol{R}\right)\\ &+\frac{m\mu}{q}\left(\mathrm{d}\zeta-\left(\boldsymbol{R}+\frac{1}{2}\tau\widehat{\mathbf{b}}\right)\cdot\mathrm{d}\mathbf{X}\right)+\mathrm{d}\sigma_2.\end{aligned} \tag{3.33}$$

where, also the gyrogauge constraint is now present. The expression could be easily simplified by choosing the functions $G_{1,\parallel}^{\mathbf{X}}$, G_1^{μ}, G_1^{ζ}, and $\boldsymbol{G}_{2,\perp}^{\mathbf{X}}$ so that the components inside the parentheses would vanish. That choice, however, is not the preferred one. Before a proper choice can be made, also the guiding center Hamiltonian has to be considered.

The total guiding center Lagrangian one-form is

$$\Gamma_{gc} - H_{gc}\mathrm{d}t = \epsilon^{-1}\Gamma_0 + \Gamma_1 + \epsilon\Gamma_2 + ... - (\mathcal{H}_0 + \epsilon\mathcal{H}_1 + ...)\,\mathrm{d}t, \tag{3.34}$$

where $H_{gc} = \mathcal{T}_{gc}^{-1}H = (1 - \epsilon\mathcal{L}_{\boldsymbol{G}_1} + ...)H$, and one can identify that each pair $(\Gamma_{i+1}, \mathcal{H}_i)$ has to be independent of the gyro-angle ζ simultaneously. In the zeroth order, the transformed Hamiltonian is simply the particle Hamiltonian evaluated at the guiding center position, namely

$$\mathcal{H}_0 = \frac{m}{2}v_\parallel^2 + \mu B, \tag{3.35}$$

and has no ζ dependence as assumed. The first order guiding center correction, $\mathcal{H}_1$, however, is defined in terms of the generating functions according to

$$\begin{aligned}\mathcal{H}_1 =& -\mathcal{L}_{\boldsymbol{G}_1}H\\ =& mv_\parallel G_1^{v_\parallel} + G_1^{\mu}B + \mu\boldsymbol{G}_1^{\mathbf{X}}\cdot\nabla B\\ =& mv_\parallel G_1^{v_\parallel} + G_1^{\mu}B + \mu B\left(G_{1,\parallel}^{\mathbf{X}}\widehat{\mathbf{b}} - \boldsymbol{\rho}_0\right)\cdot\nabla\ln B,\end{aligned} \tag{3.36}$$

and needs to be independent of ζ simultaneously with Γ_2. If the choice, setting Γ_2 trivially free of ζ, had been made, $\mathcal{H}_1$ would not have been independent of ζ.

Investigating both $\mathcal{H}_1$ and Γ_2 simultaneously reveals that the choice $G_{1,\parallel}^{\mathbf{X}} = 0$ is fine. Furthermore, because the term in Γ_2 that involves $G_1^{v_\parallel}$ is linearly independent of the the terms that involve G_1^{μ}, G_1^{ζ}, or $\boldsymbol{G}_2^{\mathbf{X}}$, i.e.,

the perpendicular velocity vector rotates in a plane perpendicular to the magnetic field, one can choose

$$G_1^{v_\parallel} = \frac{\mu}{q}(\mathbf{a}_1 : \nabla\widehat{\mathbf{b}} + \tau) - v_\parallel \boldsymbol{\rho}_0 \cdot \boldsymbol{\kappa}. \tag{3.37}$$

Then, the easiest choice for $\mathcal{H}_1$ to be independent of ζ is to set $\mathcal{H}_1 = 0$. This choice gives the condition

$$G_1^{\mu} = \mu\boldsymbol{\rho}_0 \cdot \nabla \ln B - \frac{m v_\parallel}{B} G_1^{v_\parallel}, \tag{3.38}$$

and has also the benefit that, as the first order correction to the guiding center energy is zero, the guiding center and particle energies are equal up to first order.

The final form for Γ_2 is obtained by first noting the identities

$$\frac{\partial \mathbf{v}_\perp}{\partial \zeta} = -\frac{q\mathbf{B}}{m} \times \frac{\partial \boldsymbol{\rho}_0}{\partial \zeta}, \qquad \frac{\partial \mathbf{v}_\perp}{\partial \mu} = -\frac{q\mathbf{B}}{m} \times \frac{\partial \boldsymbol{\rho}_0}{\partial \mu}, \qquad \frac{\partial \boldsymbol{\rho}_0}{\partial \zeta} = -\widehat{\mathbf{b}} \times \boldsymbol{\rho}_0 \tag{3.39}$$

and then choosing the perpendicular component of $\boldsymbol{G}_2^{\mathbf{X}}$ to be

$$\boldsymbol{G}_{2,\perp}^{\mathbf{X}} = \frac{\tau v_\parallel}{\Omega}\boldsymbol{\rho}_0 + \frac{1}{2}\left(G_1^{\zeta} + \boldsymbol{\rho}_0 \cdot \boldsymbol{R}\right)\frac{\partial \boldsymbol{\rho}_0}{\partial \zeta} + \frac{1}{2}\left(G_1^{\mu} - \mu\boldsymbol{\rho}_0 \cdot \nabla \ln B\right)\frac{\partial \boldsymbol{\rho}_0}{\partial \mu}, \tag{3.40}$$

which, together with $\sigma_2 = 0$, finally yields

$$\Gamma_2 = \frac{m\mu}{q}\left(\mathrm{d}\zeta - \boldsymbol{R}^\star \cdot \mathrm{d}\mathbf{X}\right), \tag{3.41}$$

where $\boldsymbol{R}^\star = \boldsymbol{R} + (\tau/2)\widehat{\mathbf{b}}$. The only first-order component that has not been assigned yet is G_1^{ζ} but, as all linearly independent equations have already been used, obtaining an expression for G_1^{ζ} would require the perturbation analysis to be continued up to third order. The third order analysis would determine an expression also for $G_{2,\parallel}^{\mathbf{X}}$ but, as the analysis turns out to be a rather laborous task, only the results will be given when the outcome of the Lie-transformations is summarized. An interested reader can, of course, consult Ref. [32] for the details of the third order analysis.

3.3 Summary of the Lie-transformation results

The perturbation analysis has resulted in a guiding center Lagrangian one-form

$$\Gamma = \left(\epsilon^{-1} q\mathbf{A} + m v_\parallel \widehat{\mathbf{b}} - \epsilon \frac{m\mu}{q}\boldsymbol{R}^\star\right) \cdot \mathrm{d}\mathbf{X} + \epsilon \frac{m\mu}{q}\mathrm{d}\zeta - H_{gc}\mathrm{d}t, \tag{3.42}$$

where the guiding center Hamiltonian is

$$H_{gc} = \frac{m v_\parallel^2}{2} + \mu B. \tag{3.43}$$

The procedure gave also the first order generating vector field

$$\boldsymbol{G}_1^{\mathbf{X}} = -\boldsymbol{\rho}_0 = -\frac{1}{\Omega}\sqrt{\frac{2\mu B}{m}}\widehat{\boldsymbol{\rho}}, \tag{3.44}$$

$$G_1^{v_\parallel} = \frac{\mu}{q}(\mathbf{a}_1 : \nabla\widehat{\mathbf{b}} + \tau) - v_\parallel \boldsymbol{\rho}_0 \cdot \boldsymbol{\kappa}, \tag{3.45}$$

$$G_1^{\mu} = \boldsymbol{\rho}_0 \cdot \left(\mu\nabla \ln B + \frac{m v_\parallel^2}{B}\boldsymbol{\kappa}\right) - \frac{\mu v_\parallel}{\Omega}(\mathbf{a}_1 : \nabla\widehat{\mathbf{b}} + \tau), \tag{3.46}$$

$$G_1^{\zeta} = -\boldsymbol{\rho}_0 \cdot \boldsymbol{R} + \frac{\partial \boldsymbol{\rho}_0}{\partial \zeta} \cdot \nabla \ln B + \frac{v_\parallel}{\Omega}\mathbf{a}_2 : \nabla\widehat{\mathbf{b}} + \frac{m v_\parallel^2}{2\mu B}\widehat{\mathbf{b}} \cdot \nabla\widehat{\mathbf{b}} \cdot \frac{\partial \boldsymbol{\rho}_0}{\partial \zeta}, \tag{3.47}$$

and the spatial component for the second order generating vector field

$$G_{2,\parallel}^{\mathbf{X}} = 2\frac{v_\parallel}{\Omega}\frac{\partial \boldsymbol{\rho}_0}{\partial \zeta} \cdot \boldsymbol{\kappa} + \frac{\mu}{q\Omega}\mathbf{a}_2 : \nabla\widehat{\mathbf{b}}, \tag{3.48}$$

$$\boldsymbol{G}_{2,\perp}^{\mathbf{X}} = \frac{\tau v_\parallel}{\Omega}\boldsymbol{\rho}_0 + \frac{1}{2}\left(G_1^{\zeta} + \boldsymbol{\rho}_0 \cdot \boldsymbol{R}\right)\frac{\partial \boldsymbol{\rho}_0}{\partial \zeta} + \frac{1}{2}\left(G_1^{\mu} - \mu\boldsymbol{\rho}_0 \cdot \nabla \ln B\right)\frac{\partial \boldsymbol{\rho}_0}{\partial \mu}, \tag{3.49}$$

where $\boldsymbol{R}^\star = \boldsymbol{R} + (\tau/2)\widehat{\mathbf{b}}$, $\boldsymbol{R} = \nabla\widehat{\perp} \cdot \widehat{\boldsymbol{\rho}}$ is the Littlejohn's gyrogauge field, $\tau = \widehat{\mathbf{b}} \cdot \nabla \times \widehat{\mathbf{b}}$ is the magnetic field-line twist, $\boldsymbol{\kappa} = \widehat{\mathbf{b}} \cdot \nabla\widehat{\mathbf{b}}$ is the magnetic field-line curvature vector, and the dyads $\mathbf{a}_1$ and $\mathbf{a}_2$ are defined

$$\mathbf{a}_1 = -\frac{1}{2}(\widehat{\perp}\widehat{\boldsymbol{\rho}} + \widehat{\boldsymbol{\rho}}\widehat{\perp}) = \frac{\partial \mathbf{a}_2}{\partial \zeta}, \tag{3.50}$$

$$\mathbf{a}_2 = \frac{1}{4}(\widehat{\perp}\widehat{\perp} - \widehat{\boldsymbol{\rho}}\widehat{\boldsymbol{\rho}}) = -\frac{1}{4}\frac{\partial \mathbf{a}_1}{\partial \zeta}. \tag{3.51}$$

These result will be used for constructing the guiding center kinetic equation. The Hamiltonian evolution of the guiding center motion will be obtained calculating the guiding center Poisson bracket with the given Lagrangian one-form. The collisional contribution will be obtained by carrying out the guiding center transformation of the particle Fokker-Planck term by transforming the particle phase space Poisson bracket into the guiding center phase space. The generating vectors fields will be used to calculate the gyroangle averages for the reduced guiding center Coulomb collision operator.

3.4 Hamiltonian equations of motion

The equations describing the Hamiltonian guiding center motion are obtained in a manner described in Sec. 2.3. The minimization of the action integral leads to the Lagrange matrix, the inversion of Lagrange matrix to the Poisson matrix, and the Poisson matrix to the Poisson bracket and to the equations of motion:

$$\dot{Z}^\alpha = \Pi_{gc}^{\alpha\beta}\frac{\partial H_{gc}}{\partial Z^\beta} = \{Z^\alpha, H_{gc}\}_{gc}. \tag{3.52}$$

The two-form $\mathrm{d}\Gamma_{gc}$, needed for constructing the Lagrange matrix, is calculated from the symplectic part of the guiding center Lagrangian one-form and is given by

$$\begin{aligned}\mathrm{d}\Gamma_{gc} =&\frac{q}{\epsilon}\frac{1}{2}\left(\frac{\partial A_j^\star}{\partial \mathrm{X}^\mathrm{i}}-\frac{\partial A_i^\star}{\partial \mathrm{X}^\mathrm{j}}\right)\mathrm{dX}^\mathrm{i}\wedge\mathrm{dX}^\mathrm{j}+\mathrm{d}v_\parallel\wedge\left(\frac{q}{\epsilon}\frac{\partial \mathbf{A}^\star}{\partial v_\parallel}\cdot\mathrm{d}\mathbf{X}\right)\\&+\mathrm{d}\mu\wedge\left(\frac{q}{\epsilon}\frac{\partial \mathbf{A}^\star}{\partial \mu}\cdot\mathrm{d}\mathbf{X}\right)+\epsilon\frac{m}{q}\mathrm{d}\mu\wedge\mathrm{d}\zeta\\=&\epsilon^{-1}q\varepsilon_{ijk}B^{\star,k}\mathrm{dX}^\mathrm{i}\wedge\mathrm{dX}^\mathrm{j}+\mathrm{d}v_\parallel\wedge\left(m\widehat{\mathbf{b}}\cdot\mathrm{d}\mathbf{X}\right)\\&-\epsilon\mathrm{d}\frac{m\mu}{q}\wedge\left(\mathrm{d}\zeta-\boldsymbol{R}^\star\cdot\mathrm{d}\mathbf{X}\right),\end{aligned}\tag{3.53}$$

where the definition for the effective vector potential is

$$\mathbf{A}^\star=\mathbf{A}+\epsilon(mv_\parallel/q)\widehat{\mathbf{b}}-\epsilon^2(m\mu/q^2)\boldsymbol{R}^\star,\tag{3.54}$$

and $\mathbf{B}^\star=\nabla\times\mathbf{A}^\star$ is the corresponding effective magnetic field.

The Lagrange matrix for the guiding center phase space is then

$$\boldsymbol{\omega}_{gc}=\begin{pmatrix}0&\frac{q}{\epsilon}B_z^\star&-\frac{q}{\epsilon}B_y^\star&-m\widehat{\mathrm{b}}_x&\frac{\epsilon mR_x^\star}{q}&0\\\frac{q}{\epsilon}B_z^\star&0&\frac{q}{\epsilon}B_x^\star&-m\widehat{\mathrm{b}}_y&\frac{\epsilon mR_y^\star}{q}&0\\\frac{q}{\epsilon}B_y^\star&-\frac{q}{\epsilon}B_x^\star&0&-m\widehat{\mathrm{b}}_z&\frac{\epsilon mR_z^\star}{q}&0\\m\widehat{\mathrm{b}}_x&m\widehat{\mathrm{b}}_y&m\widehat{\mathrm{b}}_z&0&0&0\\-\frac{\epsilon mR_x^\star}{q}&-\frac{\epsilon mR_y^\star}{q}&-\frac{\epsilon mR_z^\star}{q}&0&0&\frac{\epsilon m}{q}\\0&0&0&0&-\frac{\epsilon m}{q}&0\end{pmatrix},\tag{3.55}$$

where $B_\parallel^\star=\mathbf{B}^\star\cdot\widehat{\mathbf{b}}$, and the guiding center Jacobian, given by the determinant of the Lagrange matrix, is $\mathcal{J}=mB_\parallel^\star$. Calulation of the inverse gives the guiding center Poisson matrix

$$\boldsymbol{\Pi}_{gc}=\begin{pmatrix}0&-\frac{\epsilon\widehat{\mathrm{b}}_z}{qB_\parallel^\star}&\frac{\epsilon\widehat{\mathrm{b}}_y}{qB_\parallel^\star}&\frac{B_x^\star}{mB_\parallel^\star}&0&\frac{\epsilon\left(\widehat{\mathbf{b}}\times\boldsymbol{R}^\star\right)_x}{qB_\parallel^\star}\\\frac{\epsilon\widehat{\mathrm{b}}_z}{qB_\parallel^\star}&0&-\frac{\epsilon\widehat{\mathrm{b}}_x}{qB_\parallel^\star}&\frac{B_y^\star}{mB_\parallel^\star}&0&\frac{\epsilon\left(\widehat{\mathbf{b}}\times\boldsymbol{R}^\star\right)_y}{qB_\parallel^\star}\\-\frac{\epsilon\widehat{\mathrm{b}}_y}{qB_\parallel^\star}&\frac{\epsilon\widehat{\mathrm{b}}_x}{qB_\parallel^\star}&0&\frac{B_z^\star}{mB_\parallel^\star}&0&\frac{\epsilon\left(\widehat{\mathbf{b}}\times\boldsymbol{R}^\star\right)_z}{qB_\parallel^\star}\\-\frac{B_x^\star}{mB_\parallel^\star}&-\frac{B_y^\star}{mB_\parallel^\star}&-\frac{B_z^\star}{mB_\parallel^\star}&0&0&-\frac{\boldsymbol{R}^\star\cdot\mathbf{B}^\star}{mB_\parallel^\star}\\0&0&0&0&0&-\frac{q}{\epsilon m}\\-\frac{\epsilon\left(\widehat{\mathbf{b}}\times\boldsymbol{R}^\star\right)_x}{qB_\parallel^\star}&-\frac{\epsilon\left(\widehat{\mathbf{b}}\times\boldsymbol{R}^\star\right)_y}{qB_\parallel^\star}&-\frac{\epsilon\left(\widehat{\mathbf{b}}\times\boldsymbol{R}^\star\right)_z}{qB_\parallel^\star}&\frac{\boldsymbol{R}^\star\cdot\mathbf{B}^\star}{mB_\parallel^\star}&\frac{q}{\epsilon m}&0\end{pmatrix},\tag{3.56}$$

and the guiding center Poisson bracket

$$\begin{aligned}\{f,g\}_{gc}=&\epsilon^{-1}\frac{q}{m}\left(\frac{\partial f}{\partial\zeta}\frac{\partial g}{\partial\mu}-\frac{\partial f}{\partial\mu}\frac{\partial g}{\partial\zeta}\right)\\&+\frac{\mathbf{B}^\star}{mB_\parallel^\star}\cdot\left(\nabla^\star f\frac{\partial g}{\partial v_\parallel}-\frac{\partial f}{\partial v_\parallel}\nabla^\star g\right)-\epsilon\frac{\widehat{\mathbf{b}}}{qB_\parallel^\star}\cdot\left(\nabla^\star f\times\nabla^\star g\right),\end{aligned}\tag{3.57}$$

where the gyrogauge-independent gradient operator is defined as $\nabla^\star = \nabla + \boldsymbol{R}^\star \partial/\partial\zeta$. With the Poisson bracket given, one finally obtains the equations of motion

$$\dot{\mathbf{X}} = \{\mathbf{X}, H_{gc}\}_{gc} = v_\parallel \frac{\mathbf{B}^\star}{B^\star_\parallel} + \epsilon \frac{\widehat{\mathbf{b}}}{qB^\star_\parallel} \times \mu \nabla B, \tag{3.58}$$

$$\dot{v_\parallel} = \{v_\parallel, H_{gc}\}_{gc} = -\frac{\mu}{m} \frac{\mathbf{B}^\star}{B^\star_\parallel} \cdot \nabla B, \tag{3.59}$$

$$\dot{\mu} = \{\mu, H_{gc}\}_{gc} = 0, \tag{3.60}$$

$$\dot{\zeta} = \{\zeta, H_{gc}\}_{gc} = \epsilon^{-1}\Omega + \dot{\mathbf{X}} \cdot \boldsymbol{R}^\star, \tag{3.61}$$

where the dynamics of $\mathbf{X}$, $v_\parallel$, and μ are now disconnected from the rapid evolution of the gyroangle ζ, and μ has become a guiding center invariant.

One can also verify that all equations of motion, including the one for ζ, are gyrogauge invariant: The explicit expression for the effective magnetic field is $\mathbf{B}^\star = \mathbf{B} + \epsilon \frac{m v_\parallel}{\mu} \nabla \times \widehat{\mathbf{b}} - \epsilon^2 \frac{m\mu}{q^2} \nabla \times \boldsymbol{R}^\star$, and even if the second order term would be kept (in the first order theory it is not kept), the expression would still be gyrogauge invariant because $\nabla \times \boldsymbol{R}^{\star\prime} = \nabla \times (\boldsymbol{R}^\star + \nabla\chi) = \nabla \times \boldsymbol{R}^\star$. Also the equation for the gyroangle is gyrogauge invariant because when the transformation $\zeta \to \zeta + \chi$ is applied, $\dot{\zeta}' - \dot{\mathbf{X}} \cdot \boldsymbol{R}^{\star\prime} = \dot{\zeta} + \dot{\mathbf{X}} \cdot \nabla\chi - \dot{\mathbf{X}} \cdot (\boldsymbol{R}^\star + \nabla\chi) = \dot{\zeta} - \dot{\mathbf{X}} \cdot \boldsymbol{R}^\star$.

3.5 Guiding center kinetic equation

Armed with the guiding center Poisson bracket and the equations of motion, the particle kinetic equation can now be transformed into the guiding center phase space. Here, the basic principles of the transformation are discussed and accompanied with examples that help to understand the process.

As was argumented in Sec. 3.1, the coordinate transformations $\mathcal{T}_{gc} : z^\alpha \to Z^\alpha$ and $\mathcal{T}_{gc}^{-1} : Z^\alpha \to z^\alpha$ can be used to transform any scalar field f defined in phase space $\boldsymbol{z}$, to a scalar field F defined in phase space $\boldsymbol{Z}$ according to

$$F(\boldsymbol{Z}) = (\mathcal{T}_{gc}^{-1} f)(\boldsymbol{Z}) = (\mathcal{T}_{gc}^{-1} f)(\mathcal{T}_{gc}\boldsymbol{z}) = f(\boldsymbol{z}). \tag{3.62}$$

Thus, a guiding center transformation of a scalar operator $L : f \to Lf$ can be defined according to

$$\mathcal{T}_{gc}^{-1}(Lf)(\boldsymbol{z}) = (\mathcal{T}_{gc}^{-1} L) f(\boldsymbol{z}) = (L_{gc} F)(\boldsymbol{Z}), \tag{3.63}$$

where $L_{gc} = \mathcal{T}_{gc}^{-1} L$ is the guiding center transformation of the particle operator L. The particle kinetic equation derived in Sec. 2.1 was originally expressed in phase space divergence form but, later, both the Hamiltonian and collisional parts were expressed in terms of the particle Poisson bracket according to

$$\frac{\partial f}{\partial t} + \{f, H\} = \{x^i, mK^i f - m^2 D^{ij}\{x^j, f\}\}. \tag{3.64}$$

Here the indices i, j refer to Cartesian components of a vector and summation over repeated indices is assumed. As the guiding center transformation of the Poisson bracket now exists, the guiding center transformation of the kinetic equation is carried out according to the rule (3.63) to give

$$\frac{\partial F}{\partial t} + \{F, H_{gc}\}_{gc} = \{T_{gc}^{-1} x^i, m(T_{gc}^{-1} K^i)F - m^2 (T_{gc}^{-1} D^{ij})\{T_{gc}^{-1} x^j, F\}_{gc}\}_{gc}, \tag{3.65}$$

where F is now the guiding center distribution function. A far more useful presentation is obtained if Eq. (2.34) is used to transform the Poisson brackets into phase space divergence form, and the kinetic equation is expressed as

$$\frac{\partial F}{\partial t} + \dot{Z}^\alpha \frac{\partial F}{\partial Z^\alpha} = -\frac{1}{\mathcal{J}} \frac{\partial}{\partial Z^\alpha} \left[\mathcal{J} \left(m\mathcal{K}^\alpha F - m^2 \mathcal{D}^{\alpha\beta} \frac{\partial F}{\partial Z^\beta} \right) \right] = C_{gc}[F], \tag{3.66}$$

where the guiding center friction and diffusion coefficients, $\mathcal{K}^\alpha$ and $\mathcal{D}^{\alpha\beta}$, are

$$\mathcal{K}^\alpha = (\mathcal{T}_{gc}^{-1} \mathbf{K}) \cdot \boldsymbol{\Delta}^\alpha, \tag{3.67}$$

$$\mathcal{D}^{\alpha\beta} = (\boldsymbol{\Delta}^\alpha)^\dagger \cdot (\mathcal{T}_{gc}^{-1} \mathbf{D}) \cdot \boldsymbol{\Delta}^\beta, \tag{3.68}$$

and the projection vectors $\boldsymbol{\Delta}^\alpha$ are defined in terms of the guiding center Poisson tensor

$$\boldsymbol{\Delta}^\alpha = -\Pi^{\alpha\beta} \frac{\partial}{\partial Z^\beta} \mathcal{T}_{gc}^{-1} \mathbf{x} = \hat{\boldsymbol{e}}^i \{\mathcal{T}_{gc}^{-1} x^i, Z^\alpha\} \equiv \{\mathcal{T}_{gc}^{-1} \mathbf{x}, Z^\alpha\}. \tag{3.69}$$

Here $\hat{\boldsymbol{e}}^i$ refers to the Cartesian unit vectors. One should note that, as the result includes spatial derivatives, the collisional term now introduces spatial drag and diffusion that were not present in the particle collision operator that acted solely in the particle velocity space. The spatial components only reflect the results of the coordinate transformation which is illustrated in Fig. 3.1.

The kinetic equation as expressed by (3.66) describes the time evolution of the guiding center distribution function in phase space $(\mathbf{X}, v_\parallel, \mu, \zeta)$ that includes the rapidly changing gyroangle ζ. As such, it offers little if

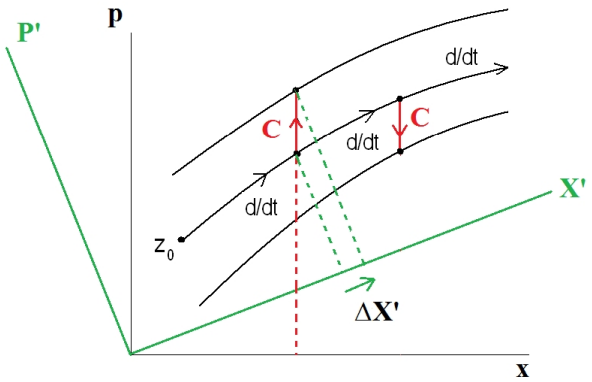

Figure 3.1. A Schematic view of Coulomb collision after coordinate transformation. Here the time derivative denotes the Hamiltonian motion and the red C the Coulomb collisions. The transformation from particle coordinates $\mathbf{x}, \mathbf{p}$ into guiding center coordinates $\mathbf{X}', \mathbf{P}'$ introduces a spatial change $\Delta\mathbf{X}'$ in the guiding center position. Courtesy of Alain Brizard.

no benefit at all compared to the particle phase space. If, however, the guiding center distribution function F is written as a sum

$$F = \langle F \rangle + \tilde{F} \tag{3.70}$$

where $\langle F \rangle$ is the gyroangle average of F and $\tilde{F} = F - \langle F \rangle$ is the residual term, the fact that the Hamiltonian motion of the coordinates $\mathbf{X}, v_\parallel, \mu$ is independent of ζ makes it possible to write the guiding center kinetic equation as two coupled equations, namely

$$\frac{d_{\boldsymbol{R}}}{dt}\langle F \rangle = \langle C_{gc}[F] \rangle = \langle C_{gc}[\langle F \rangle] \rangle + \langle C_{gc}[\tilde{F}] \rangle, \tag{3.71}$$

$$\frac{d_{\boldsymbol{R}}}{dt}\tilde{F} + \dot{\zeta}\frac{\partial \tilde{F}}{\partial \zeta} = C_{gc}[F] - \langle C_{gc}[F] \rangle, \tag{3.72}$$

where the reduced guiding center Vlasov operator is defined as

$$\frac{d_{\boldsymbol{R}}}{dt} = \left(\frac{\partial}{\partial t} + \dot{\mathbf{X}} \cdot \nabla + \dot{v_\parallel} \frac{\partial}{\partial v_\parallel} \right). \tag{3.73}$$

The equation for $\langle F \rangle$ is still dependent on the fast gyroangle via the coupling term $\langle C_{gc}[\tilde{F}] \rangle$ but, as is explained in [40], if an approximate solution of Eq. (3.72) is submitted into Eq. (3.71), the result will be

$$\frac{d_{\boldsymbol{R}}}{dt}\langle F \rangle = \langle C_{gc}[\langle F \rangle] \rangle + \mathcal{O}(\epsilon_\nu), \tag{3.74}$$

where the small parameter $\epsilon_\nu = \nu/\Omega$ is the ratio of the characteristic collision rate ν and the gyro frequency Ω.

In collisional kinetic theory [49] the ratio $\Delta = \epsilon_B/\epsilon_\nu$ is used to categorize the different collisional regimes and, e.g., the classical collisional regime,

where collisions dominate the magnetic field nonuniformity, is characterized by $\Delta \ll 1$. In neoclassical collisionless regime, which is highly relevant for the tokamaks, one has $\Delta \gg 1$. As the Vlasov part of the kinetic equation is characterized by the magnetic field nonuniformity (ϵ_B) that appears in the equations of motion, and because $\epsilon_\nu = \epsilon_B/\Delta$, it is justified to include only the lowest order collision term in the equation for $\langle F \rangle$, so that the reduced guiding center kinetic equation in the neoclassical regime becomes

$$\frac{\partial \langle F \rangle}{\partial t} + \dot{Z}^\alpha \frac{\partial \langle F \rangle}{\partial Z^\alpha} = -\frac{1}{\mathcal{J}} \frac{\partial}{\partial Z^\alpha} \left[\mathcal{J} \left(m \langle \mathcal{K}^\alpha \rangle \langle F \rangle - m^2 \langle \mathcal{D}^{\alpha\beta} \rangle \frac{\partial \langle F \rangle}{\partial Z^\beta} \right) \right], \quad (3.75)$$

where $Z^\alpha = (\mathbf{X}, v_\parallel, \mu)$ is now the reduced guiding center phase space, and $\langle F \rangle$ is the distribution function in the reduced guiding center phase space. From here on, the notation $\langle F \rangle$ is dropped, and F refers to the reduced guiding center distribution function.

3.6 Guiding center Coulomb drag and diffusion coefficients

Before presenting the stochastic differential equation that describes the Hamiltonian and collisional guiding center motion, the gyroaverages for the guiding center Coulomb drag, $m\langle \mathcal{K}^\alpha \rangle = \mathcal{K}^\alpha_{gc}$, and diffusion, $m^2 \langle \mathcal{D}^{\alpha\beta} \rangle = \mathcal{D}^{\alpha\beta}_{gc}$, are needed. Instead of calculating the coefficients directly for the phase space $(\mathbf{X}, v_\parallel, \mu)$ where the equations of motion are given, the coefficients for a phase space $(\mathbf{X}, \mathcal{E}, \mu)$, originally calculated in Ref. [40], are transformed into the desired phase space, as is done in Publication III. To give an example of the averaging procedure, the calculation of $\mathcal{K}^{\mathbf{X}}_{gc}$ is presented explicitly.

Evaluation of the expression

$$\mathcal{K}^{\mathbf{X}}_{gc} = \mathcal{K}^i_{gc} \widehat{\mathbf{e}}^i = -m \langle \mathcal{T}^{-1}_{gc} \mathbf{K} \cdot \boldsymbol{\Delta}^i \rangle \widehat{\mathbf{e}}^i = -m \langle \widehat{\mathbf{e}}^i \boldsymbol{\Delta}^i \cdot \mathcal{T}^{-1}_{gc} \mathbf{v} \mathcal{T}^{-1}_{gc} \nu \rangle, \quad (3.76)$$

requires the spatial projection dyad $\widehat{\mathbf{e}}^i \boldsymbol{\Delta}^i$, together with the guiding center transformations of the particle friction rate, $\mathcal{T}^{-1}_{gc}\nu$, and the particle velocity, $\mathcal{T}^{-1}_{gc}\mathbf{v}$. The transformation of the friction rate becomes simple because, in the particle phase space, it is only a function of the particle energy. As discussed during the derivation of the guiding center Lagrangian one form, the particle energy matches the guiding center energy up to first order in ϵ and, thus, one has

$$\mathcal{T}^{-1}_{gc}\nu = \nu + \mathcal{O}(\epsilon^2). \quad (3.77)$$

For the transformation of the particle velocity, one first notes that the velocity is a time derivative of the position. Therefore, one can apply the transformation rule given in Eq. (3.63) and write the guiding center transformed particle velocity as

$$\begin{aligned}\mathcal{T}_{gc}^{-1}\mathbf{v} =& \left(\mathcal{T}_{gc}^{-1}\frac{d}{dt}\right)\left(\mathbf{X}+\epsilon\boldsymbol{\rho}_0+\epsilon^2\boldsymbol{\rho}_1\right)\\ =&\dot{\mathbf{X}}+\left(\dot{\mathbf{X}}\cdot\nabla+\dot{v_\parallel}\frac{\partial}{\partial v_\parallel}+\dot{\zeta}\frac{\partial}{\partial\zeta}\right)\left(\epsilon\boldsymbol{\rho}_o+\epsilon^2\boldsymbol{\rho}_1\right)\\ =&\dot{\mathbf{X}}+\Omega\frac{\partial\boldsymbol{\rho}_0}{\partial\zeta}+\epsilon\left(v_\parallel\widehat{\mathbf{b}}\cdot\nabla^\star\boldsymbol{\rho}_0+\Omega\frac{\partial\boldsymbol{\rho}_1}{\partial\zeta}\right)+\mathcal{O}(\epsilon^2).\end{aligned} \tag{3.78}$$

Here, also the second order correction, $\boldsymbol{\rho}_1$, is needed because the equation of motion for ζ involves a term $\epsilon^{-1}\Omega$. The spatial projection dyad is evaluated with the help of the Poisson tensor giving

$$\begin{aligned}\widehat{\mathbf{e}}^i\boldsymbol{\Delta}^i =& -\widehat{\mathbf{e}}^i\Pi^{i\beta}\frac{\partial}{\partial Z^\beta}\left(\mathbf{X}+\epsilon\boldsymbol{\rho}_0+\epsilon^2\boldsymbol{\rho}_1+...\right)\\ =& -\epsilon\frac{\widehat{\mathbf{b}}}{qB_\parallel^\star}\times\mathbf{I}-\epsilon^2\frac{\widehat{\mathbf{b}}}{qB_\parallel^\star}\times\nabla^\star\boldsymbol{\rho}_0-\epsilon^2\frac{\Omega}{qB_\parallel^\star}\widehat{\mathbf{b}}\frac{\partial\boldsymbol{\rho}_1}{\partial v_\parallel}+\mathcal{O}(\epsilon^3),\end{aligned} \tag{3.79}$$

and the spatial component for the guiding center friction vector becomes

$$\begin{aligned}\mathcal{K}_{gc}^{\mathbf{X}} =&\epsilon\frac{m\nu\widehat{\mathbf{b}}}{qB_\parallel^\star}\times\left(\dot{\mathbf{X}}+\Omega\langle\frac{\partial\boldsymbol{\rho}_0}{\partial\zeta}\rangle+\epsilon v_\parallel\widehat{\mathbf{b}}\cdot\langle\nabla^\star\boldsymbol{\rho}_0\rangle+\epsilon\Omega\langle\frac{\partial\boldsymbol{\rho}_1}{\partial\zeta}\rangle\right)\\ &+\epsilon^2\frac{m\nu\widehat{\mathbf{b}}}{qB_\parallel^\star}\times\langle\nabla^\star\boldsymbol{\rho}_0\cdot\left(\dot{\mathbf{X}}+\Omega\frac{\partial\boldsymbol{\rho}_0}{\partial\zeta}\right)\rangle\\ &+\epsilon^2\frac{m\nu}{qB_\parallel^\star}\Omega\widehat{\mathbf{b}}\langle\frac{\partial\boldsymbol{\rho}_1}{\partial v_\parallel}\cdot\left(\dot{\mathbf{X}}+\Omega\frac{\partial\boldsymbol{\rho}_0}{\partial\zeta}\right)\rangle+\mathcal{O}(\epsilon^3).\end{aligned} \tag{3.80}$$

The gyroaverages $\langle\frac{\partial\boldsymbol{\rho}_0}{\partial\zeta}\rangle$, $\langle\nabla^\star\boldsymbol{\rho}_0\rangle$, and $\langle\frac{\partial\boldsymbol{\rho}_1}{\partial\zeta}\rangle$ are zero. The gyro-average needed for the second last term,

$$\langle\nabla^\star\boldsymbol{\rho}_0\cdot\frac{\partial\boldsymbol{\rho}_0}{\partial\zeta}\rangle=\frac{\rho_o^2\tau}{2}\widehat{\mathbf{b}}, \tag{3.81}$$

is non-zero, but as this term is crossed with the magnetic field unit vector, the contribution to the spatial friction vector is zero. The last term requires the expression for $\boldsymbol{\rho}_1$, which essentially is the second order term in $\mathcal{T}_{gc}^{-1}\mathrm{x}$. By definition of $\mathcal{T}_{gc}^{-1}$, one has

$$\begin{aligned}\boldsymbol{\rho}_1 =&\left(\frac{1}{2}\mathcal{L}_{\boldsymbol{G}_1}^2-\mathcal{L}_{\boldsymbol{G}_2}\right)\mathbf{X}\\ =& -G_2^{\mathbf{X}}-\frac{1}{2}G_1^\zeta\frac{\partial\boldsymbol{\rho}_0}{\partial\zeta}-\frac{1}{2}G_1^\mu\frac{\partial\boldsymbol{\rho}_0}{\partial\mu}+\frac{1}{2}\boldsymbol{\rho}_0\cdot\nabla\boldsymbol{\rho}_0,\end{aligned} \tag{3.82}$$

and since $\boldsymbol{\rho}_0$ is independent of $v_\parallel$, and $\frac{\partial\boldsymbol{\rho}_0}{\partial\zeta}$ is perpendicular to $\frac{\partial\boldsymbol{\rho}_0}{\partial\mu}$, we have

$$\begin{aligned}\frac{\partial\boldsymbol{\rho}_1}{\partial v_\parallel}\cdot\left(\dot{\mathbf{X}}+\Omega\frac{\partial\boldsymbol{\rho}_0}{\partial\zeta}\right) =&\frac{\partial\boldsymbol{G}_2^{\mathbf{X}}}{\partial v_\parallel}\cdot\left(v_\parallel\widehat{\mathbf{b}}+\Omega\frac{\partial\boldsymbol{\rho}_0}{\partial\zeta}\right)-\frac{1}{2}\frac{\partial G_2^\zeta}{\partial v_\parallel}\rho_0^2\Omega,\\ =& -\frac{2v_\parallel}{\Omega}\frac{\partial\boldsymbol{\rho}_0}{\partial\zeta}\cdot\boldsymbol{\kappa}-\rho_0^2\mathbf{a}_2:\nabla\widehat{\mathbf{b}}+\rho_0^2\Omega\frac{mv_\parallel}{\mu B}\widehat{\mathbf{b}}\cdot\nabla\widehat{\mathbf{b}}\cdot\frac{\partial\boldsymbol{\rho}_0}{\partial\zeta}\end{aligned} \tag{3.83}$$

Noting the relations (3.50) and (3.51), one sees that the gyro-average of the above expression is zero, and the spatial component for the guiding center friction vector becomes

$$\mathcal{K}_{gc}^{\mathbf{X}} = \epsilon \frac{\nu}{\Omega_{\parallel}^{\star}} \widehat{\mathbf{b}} \times \dot{\mathbf{X}} + \mathcal{O}(\epsilon^3), \tag{3.84}$$

where $\Omega_{\parallel}^{\star} = qB_{\parallel}^{\star}/m$.

The rest of the guiding center Fokker-Planck coefficients for the $(\mathbf{X}, \mathcal{E}, \mu)$ phase-space are calculated in Ref. [40]. The explicit expressions for the collisional (isotropic) diffusion coefficients are

$$\mathcal{D}_{gc}^{\mathbf{X}\mathbf{X}} = \epsilon^2 \left[(D_{\parallel} - D_{\perp}) \frac{\mu B}{2\mathcal{E}} + D_{\perp} \right] \frac{\mathbf{I} - \widehat{\mathbf{b}}\widehat{\mathbf{b}}}{(m\Omega_{\parallel}^{\star})^2} + \mathcal{O}(\epsilon^3), \tag{3.85}$$

$$\mathcal{D}_{gc}^{\mathcal{E}\mathcal{E}} = \frac{2\mathcal{E}}{m} D_{\parallel} + \mathcal{O}(\epsilon^2), \tag{3.86}$$

$$\mathcal{D}_{gc}^{\mu\mu} = (1 - \epsilon\lambda) \frac{2\mu}{mB} \left[(D_{\parallel} - D_{\perp}) \frac{\mu B}{\mathcal{E}} + D_{\perp} \right] + \mathcal{O}(\epsilon^2), \tag{3.87}$$

$$\mathcal{D}_{gc}^{\mathbf{X}\mathcal{E}} = -\epsilon \frac{D_{\parallel}}{m} \frac{\widehat{\mathbf{b}}}{\Omega_{\parallel}^{\star}} \times \dot{\mathbf{X}} + \mathcal{O}(\epsilon^3), \tag{3.88}$$

$$\mathcal{D}_{gc}^{\mathbf{X}\mu} = -\epsilon \frac{\mu}{2m\mathcal{E}} (D_{\parallel} - D_{\perp}) \frac{\widehat{\mathbf{b}}}{\Omega_{\parallel}^{\star}} \times \dot{\mathbf{X}} + \mathcal{O}(\epsilon^3), \tag{3.89}$$

$$\mathcal{D}_{gc}^{\mathcal{E}\mu} = (2 - \epsilon\lambda) D_{\parallel} \frac{\mu}{m} + \mathcal{O}(\epsilon^2), \tag{3.90}$$

and the collisional (isotropic) friction coefficients are

$$\mathcal{K}_{gc}^{\mathbf{X}} = \epsilon\nu \frac{\widehat{\mathbf{b}}}{\Omega_{\parallel}^{\star}} \times \dot{\mathbf{X}} + \mathcal{O}(\epsilon^3), \tag{3.91}$$

$$\mathcal{K}_{gc}^{\mathcal{E}} = -2\nu\mathcal{E} + \mathcal{O}(\epsilon^2), \tag{3.92}$$

$$\mathcal{K}_{gc}^{\mu} = -(2 - \epsilon\lambda)\nu\mu + \mathcal{O}(\epsilon^2), \tag{3.93}$$

where in Eqs. (3.87), (3.90) and (3.93), $\lambda = v_{\parallel}\tau/\Omega$ is related to the magnetic field-line twist.

To calculate the guiding-center friction and diffusion coefficients for the phase-space $(\mathbf{X}, v_{\parallel}, \mu)$, the chain rule for a Poisson bracket, $\{F, \mathcal{Z}^{\beta}\} = \{F, \mathcal{Z}^{\alpha}\} \frac{\partial \mathcal{Z}^{\beta}}{\partial \mathcal{Z}^{\alpha}}$, is used which allows the new projection vectors to be written in terms of the old ones according to $\mathbf{\Delta}^{\beta} = \mathbf{\Delta}^{\alpha} \frac{\partial \mathcal{Z}^{\beta}}{\partial \mathcal{Z}^{\alpha}}$, and to obtain

$$\mathcal{K}_{gc}^{\alpha} = \mathcal{K}_{gc}^{\gamma} \frac{\partial \mathcal{Z}^{\alpha}}{\partial \mathcal{Z}^{\gamma}}, \tag{3.94}$$

$$\mathcal{D}_{gc}^{\alpha\beta} = \frac{\partial \mathcal{Z}^{\alpha}}{\partial \mathcal{Z}^{\gamma}} \mathcal{D}_{gc}^{\gamma\delta} \frac{\partial \mathcal{Z}^{\beta}}{\partial \mathcal{Z}^{\delta}}. \tag{3.95}$$

It is then a simple task to calculate the partial derivatives between phase-spaces $\mathcal{Z}^{\alpha} = (\mathbf{X}, v_{\parallel}, \mu)$ and $\mathcal{Z}^{\gamma} = (\mathbf{X}, \mathcal{E}, \mu)$, and to obtain, from Eqs. (3.86)-

(3.90), the new collisional diffusion coefficients

$$\mathcal{D}_{gc}^{v_\parallel v_\parallel} = \frac{D_\parallel}{m^2} + (1-\epsilon\lambda)\frac{D_\perp - D_\parallel}{m^2}\frac{\mu B}{\mathcal{E}} + \mathcal{O}(\epsilon^2), \tag{3.96}$$

$$\begin{aligned}\mathcal{D}_{gc}^{\mathbf{X}v_\parallel} = {} & \epsilon^2 \frac{v_\parallel}{(m\Omega_\parallel^\star)^2}(D_\parallel - D_\perp)\frac{\mu B}{2\mathcal{E}}\nabla_\perp \ln B \\ & + \epsilon^2 \frac{v_\parallel}{(m\Omega_\parallel^\star)^2}\left[D_\parallel + \frac{\mu B}{2\mathcal{E}}(D_\perp - D_\parallel)\right]\widehat{\mathbf{b}}\cdot\nabla\widehat{\mathbf{b}} + \mathcal{O}(\epsilon^3),\end{aligned} \tag{3.97}$$

$$\mathcal{D}_{gc}^{\mu v_\parallel} = (1-\epsilon\lambda)\frac{\mu v_\parallel}{m\mathcal{E}}(D_\parallel - D_\perp) + \epsilon\lambda\frac{\mu}{v_\parallel m^2}D_\parallel + \mathcal{O}(\epsilon^2), \tag{3.98}$$

where $\nabla_\perp = (\mathbf{I} - \widehat{\mathbf{b}}\widehat{\mathbf{b}})\cdot\nabla$, as well as, from Eqs. (3.92)-(3.93) the new friction coefficient

$$\mathcal{K}_{gc}^{v_\parallel} = -\nu v_\parallel - \epsilon\lambda\frac{\mu B}{m v_\parallel}\nu + \mathcal{O}(\epsilon^2), \tag{3.99}$$

The other coefficients for $\mathcal{D}_{gc}^{\mathbf{XX}}$, $\mathcal{D}_{gc}^{\mathbf{X}\boldsymbol{\mu}}$, etc. remain unchanged.

3.7 Stochastic differential equation for a guiding center

The guiding center kinetic equation as it now stands

$$\frac{\partial F}{\partial t} + \dot{Z}^\alpha \frac{\partial F}{\partial Z^\alpha} = -\frac{1}{\mathcal{J}}\frac{\partial}{\partial Z^\alpha}\left[\mathcal{J}\left(\mathcal{K}_{gc}^\alpha F - \mathcal{D}_{gc}^{\alpha\beta}\frac{\partial F}{\partial Z^\beta}\right)\right], \tag{3.100}$$

is not yet in a similar form as the particle kinetic equation was when the connection to the stochastic differential equation was established. The connection can be obtained, though, if the equations of motion appearing in the guiding center kinetic equation are written in the divergence form, and the diffusion term is written in two parts as was done in Publication III. As a result, the guiding center kinetic equation can be written as

$$\frac{\partial \mathcal{F}}{\partial t} = -\frac{1}{\mathcal{J}}\frac{\partial}{\partial \mathcal{Z}^\alpha}\left(\mathcal{J}\mathcal{A}^\alpha \mathcal{F}\right) + \frac{1}{\mathcal{J}}\frac{\partial^2}{\partial \mathcal{Z}^\alpha \partial \mathcal{Z}^\beta}\left(\mathcal{J}\mathcal{D}^{\alpha\beta}\mathcal{F}\right), \tag{3.101}$$

where the coefficient $\mathcal{A}^\alpha$ is

$$\mathcal{A}^\alpha = \dot{\mathcal{Z}}^\alpha + \mathcal{K}^\alpha + \frac{1}{\mathcal{J}}\frac{\partial}{\partial \mathcal{Z}^\beta}(\mathcal{J}\mathcal{D}^{\alpha\beta}). \tag{3.102}$$

The stochastic differential equation for a phase-space coordinate $\mathcal{Z}^\alpha$ thus becomes

$$d\mathcal{Z}^\alpha = \mathcal{A}_{gc}^\alpha dt + \Sigma_{gc}^{\alpha\beta} d\mathcal{W}^\beta, \tag{3.103}$$

where the matrix $\Sigma_{gc}^{\alpha\beta}$ satisfies

$$\mathcal{D}_{gc}^{\alpha\beta} = \frac{1}{2}\Sigma_{gc}^{\alpha\gamma}\Sigma_{gc}^{\beta\gamma}, \tag{3.104}$$

and $\mathcal{W}^\alpha$ are independent standard Wiener processes with zero mean and variance t.

In particle phase-space, it was straight-forward to obtain the matrix $\sigma^{\alpha\beta}$ because the diffusion matrix could be easily diagonalized. In guiding-center phase-space, the decomposition of $\mathcal{D}_{gc}^{\alpha\beta}$, however, is not trivial. Use of the eigenvalue decomposition, for example, requires that the units of the components of $\mathcal{D}^{\alpha\beta}$ are equal. In Publication III, it was discussed how the decomposition is carried out by writing the diffusion matrix as a product of three matrices

$$\mathcal{D}_{gc}^{\alpha\beta} = \mathcal{B}^{\alpha\gamma}\mathcal{Y}^{\gamma\nu}\mathcal{B}^{\nu\beta}, \tag{3.105}$$

where $\mathcal{B}^{\alpha\beta}$ is a diagonal matrix defined so that the entries of $\mathcal{Y}^{\alpha\beta}$ have equal units, and the eigenvalue decomposition is then conducted for the matrix $\mathcal{Y}^{\alpha\beta}$. In principle, the components of $\mathcal{B}^{\alpha\beta}$ could be arbitrary, as long as the units match the requirements but, in Publication III, the choice was

$$\mathcal{B}^{\alpha\beta} = \begin{pmatrix} |\mathbf{X}|\mathbf{I} & \mathbf{0} \\ \mathbf{0} & \begin{pmatrix} v & 0 \\ 0 & \mathcal{E}/B \end{pmatrix} \end{pmatrix}, \tag{3.106}$$

which yielded the normalized matrix components

$$\mathcal{Y}^{\alpha\beta} = \begin{pmatrix} \frac{\mathcal{D}^{\mathbf{X}\mathbf{X}}}{|\mathbf{X}|^2} & \frac{\mathcal{D}^{\mathbf{X}v_\parallel}}{|\mathbf{X}|v} & \frac{B}{\mathcal{E}}\frac{\mathcal{D}^{\mathbf{X}\mu}}{|\mathbf{X}|} \\ \frac{\mathcal{D}^{v_\parallel\mathbf{X}}}{|\mathbf{X}|v} & \frac{\mathcal{D}^{v_\parallel v_\parallel}}{v^2} & \frac{B}{\mathcal{E}}\frac{\mathcal{D}^{v_\parallel\mu}}{v} \\ \frac{B}{\mathcal{E}}\frac{\mathcal{D}^{\mu\mathbf{X}}}{|\mathbf{X}|} & \frac{B}{\mathcal{E}}\frac{\mathcal{D}^{v_\parallel\mu}}{v} & \frac{B^2\mathcal{D}^{\mu\mu}}{\mathcal{E}^2} \end{pmatrix}. \tag{3.107}$$

In a tokamak, the charged particle position never proceeds to the center of the global coordinate system, and the kinetic energy, velocity, and magnetic field strength are always positive quantities, making the choice reasonable.

To construct a real-valued $\Sigma_{gc}^{\alpha\beta}$ with eigenvalue decomposition, there is yet another condition the diffusion matrix must satisfy: the matrix $\mathcal{Y}^{\alpha\beta}$ has to be positive semidefinite. In Publication III, it was shown that the guiding center diffusion matrix has one eigenvalue that is zero, but an explicit proof for the matrix to be positive semidefinite was not accomplished. Clear condition, in terms of the eigenvalues, was given though. Here, the proof is provided for the first time by noting that the guiding center transformation of the particle diffusion matrix

$$\mathcal{T}_{gc}^{-1}\mathbf{D} = \mathcal{T}_{gc}^{-1}D_\parallel\frac{(\mathcal{T}_{gc}^{-1}\mathbf{v})(\mathcal{T}_{gc}^{-1}\mathbf{v})}{\mathcal{T}_{gc}^{-1}(v^2)} + \mathcal{T}_{gc}^{-1}D_\perp\left(\mathbf{I} - \frac{(\mathcal{T}_{gc}^{-1}\mathbf{v})(\mathcal{T}_{gc}^{-1}\mathbf{v})}{\mathcal{T}_{gc}^{-1}(v^2)}\right) \tag{3.108}$$

is positive semidefinite by definition, because $\mathcal{T}_{gc}^{-1}D_{\parallel}$ and $\mathcal{T}_{gc}^{-1}D_{\perp}$ are non-negative (Lie-transformation is scalar invariant). This implies that for any vector $\mathbf{x}$, one has

$$\mathbf{x}\cdot(\mathcal{T}_{gc}^{-1}\mathbf{D})\cdot\mathbf{x}\geq 0. \tag{3.109}$$

In particular, choosing $\mathbf{x}=P^{\alpha}\boldsymbol{\Delta}^{\alpha}$ gives

$$0\leq P^{\alpha}\boldsymbol{\Delta}^{\alpha}\cdot(\mathcal{T}_{gc}^{-1}\mathbf{D})\cdot\boldsymbol{\Delta}^{\beta}P^{\beta}=P^{\alpha}\mathcal{D}^{\alpha\beta}P^{\beta}. \tag{3.110}$$

Calculating the gyro-average then yields

$$0\leq\langle P^{\alpha}\mathcal{D}^{\alpha\beta}P^{\beta}\rangle=P^{\alpha}\langle\mathcal{D}^{\alpha\beta}\rangle P^{\beta}=P^{\alpha}\mathcal{D}_{gc}^{\alpha\beta}P^{\beta}, \tag{3.111}$$

and further choosing $P^{\alpha}=Q^{\alpha}/\mathcal{B}^{\alpha\alpha}$ reveals that

$$Q^{\alpha}\mathcal{Y}^{\alpha\beta}Q^{\beta}\geq 0, \tag{3.112}$$

which proves that both the gyroaveraged guiding center diffusion coefficient $\mathcal{D}_{gc}^{\alpha\beta}$ and the normalized matrix $\mathcal{Y}^{\alpha\beta}$ are positive semidefinite. This result proves that the eigenvalue decomposition will yield a real-valued matrix $\Sigma^{\alpha\beta}$, and guarantees that the stochastic differential equation for guiding center motion can be constructed.

The most evident result of the guiding center transformation of the particle collision operator is the appearance of spatial friction and diffusion in addition to the conventional velocity space transport. In Publication III, this was demostrated by making the assumption of uniform magnetic field, and giving an explicit expression for the spatial diffusion. The result

$$d\mathbf{X}=\sqrt{2D^{\mathbf{X}}}(\mathbf{I}-\widehat{\mathbf{b}}\widehat{\mathbf{b}})\cdot\mathcal{W}^{\mathbf{X}}, \tag{3.113}$$

where the spatial diffusion coefficient is given by

$$D^{\mathbf{X}}=[(D_{\parallel}-D_{\perp})\frac{\mu B}{2\mathcal{E}}+D_{\perp}]/[(m\Omega_{\parallel}^{\star})^{2}], \tag{3.114}$$

is reported also in [50]. The results presented in Publication III, however, significantly differ from the previous studies. For the first time, the collisional guiding center motion is derived consistently with the Hamiltonian motion including also the effects introduced by the magnetic field nonuniformity.

3.8 A short summary of the guiding center transformation

In this chapter, the guiding center transformation was introduced, and the rapid gyromotion present in the particle kinetic equation was isolated

into variables that are not needed in following the evolution of the guiding center kinetic equation. The isolation proceeded by first constructing the Hamiltonian motion of the guiding center phase space to be independent of the rapid gyroangle. Then, the particle kinetic equation was transformed into guiding center phase space and the rapid gyromotion was argued irrelevant for the collisional part. As a result, a theoretical description of transport is obtained for a set of coordinates that offers significant computational benefits compared to particle phase space, but manages to avoid the shortcomings of orbit averaged methods: the guiding center theory is not limited to regions of closed magnetic flux surfaces, nor to axisymmetric magnetic fields.

4. Fast ion modeling

The essential parts of the theory describing the neoclassical transport of minority populations in tokamak plasmas was presented in the previous chapters for both the particle and the guiding center phase space. However, plasmas exhibit much more complicated phenomena that affect the minority particles. These include, e.g., the turbulence and MHD activity. In this Chapter, models that mimic the effects of these two important transport mechanism are presented (see Publications I and II). The basic theory and these models are also implemented in Publication IV to construct a comprehensive numerical tool for minority particle studies. Finally, a summary of Publication V is given to demonstrate possible applications for both the theory and the code.

4.1 A model for anomalous radial diffusion

In the introduction, it was noted that the confinement in tokamaks is determined not only by neoclassical transport (see chapters 2 and 3), but also by turbulent fluctuations in the electromagnetic fields. Although it is known that turbulence plays an important role, it cannot be inherently included in minority particle studies because the evolution of the electric and magnetic fields would require simulating the entire plasma self-consistently. Thus, the effect of the turbulence on the minority population has to be approximated as an anomalous diffusive process. In Publication I, a simple method to include anomalous processes into minority particle studies was presented and, here, the publication is shortly summarized.

Assuming that an expression for a spatial diffusion coefficient D exists, and that the flux of particles across some surface obeys Fick's law, the evolution of the distribution function due to this diffusive process is given

by

$$\frac{\partial f}{\partial t} = \frac{\partial}{\partial \mathbf{x}} \cdot \left(D \frac{\partial f}{\partial \mathbf{x}} \right) = \frac{1}{\sqrt{g}} \frac{\partial}{\partial u^i} \left(\sqrt{g} D g^{ij} \frac{\partial f}{\partial u^j} \right), \tag{4.1}$$

where D is given in its natural units m^2/s, $\sqrt{g}$ is the Jacobian of the curvilinear coordinates $\mathbf{x} = (u^1, u^2, u^3)$ and the $g^{ij} = \nabla u^i \cdot \nabla u^j$ are the components of the symmetric contravariant metric tensor. The motion of a phase space coordinate u^i is then given by the stochastic differential equation

$$du^i = \frac{1}{\sqrt{g}} \frac{\partial}{\partial u^j} \left(\sqrt{g} D g^{ij} \right) dt + \sigma^{ij} d\beta^j, \tag{4.2}$$

where $\sigma^{ik}\sigma^{jk} = 2Dg^{ij}$. The matrix σ^{ij} can always be constructed with an eigenvalue decomposition of g^{ij} because the metric tensor is always positive semidefinite. If the stochastic differential equation is then integrated with the Euler method, the step in u^i is given by

$$\Delta u^i = \frac{1}{\sqrt{g}} \frac{\partial}{\partial u^j} \left(\sqrt{g} D g^{ij} \right) \Delta t + \sqrt{\Delta t} \sigma^{ij} \beta^j, \tag{4.3}$$

where β^j are now random numbers with unit variance and zero expectation, e.g., ± 1.

At the time of writing Publication I, the author was not yet aware of the connectiong between the Fokker-Planck equation and stochastic processes and, instead of expressing the motion of the coordinate u^i with Eq. (4.3), it was assumed that the motion could be described with the evolution of the expectation value and variance according to

$$\Delta u^i = \frac{d}{dt} \mathrm{E}[u^i] \Delta t \pm \sqrt{\frac{d}{dt} \mathrm{E}[(u^i - \mathrm{E}[u^i])^2] \Delta t}. \tag{4.4}$$

This assumption then gave a step

$$\Delta u^i = \frac{1}{\sqrt{g}} \frac{\partial}{\partial u^j} \left(\sqrt{g} D g^{ij} \right) \Delta t \pm \sqrt{2 D g^{ii} \Delta t}, \tag{4.5}$$

which, in general case, is wrong. Equation (4.3) clearly points out that also the off-diagonal components of the metric tensor contribute to the stochastic part. The step given by Eq. (4.5) contains only the diagonal contribution and, thus, holds only for a coordinate system which is orthogonal.

Instead of just offering an expression for the displacement Δu^i, Publication I served a deeper purpose. Back in the 1980's Boozer and Kuo-Petravic presented their famous Monte Carlo calculations of the neoclassical transport coefficients [51] in the limit of large aspect ratio (plasma is almost a straight cylinder). To determine the transport coefficient they

interpreted the motion of the test particle to be a result of a diffusion process where the displacement of the particle position in the radial direction would be given according to

$$\Delta u = \frac{1}{s}\frac{\partial}{\partial u}\left(sDg^{uu}\right)\Delta t \pm \sqrt{2Dg^{uu}\Delta t}, \tag{4.6}$$

where s is the one dimensional differential volume element according to $d\mathbf{x} = s(u)du$. This operator was then adopted in test particle codes to model anomalous processes. Now, that most of the tokamaks do not satisfy assumption of large aspect ratio, the old step given by Eq. (4.6) should not be used but, instead, the proper step is given by Eq. (4.3).

The difference between the models was explicitly shown in Publication I using simple toroidal coordinates (r, θ_p, ϕ) that relate to cylindrical coordinates (R, ϕ, z):

$$R = R_0 + r\cos\theta_p, \quad z = r\sin\theta_p. \tag{4.7}$$

The metric tensor becomes diagonal with non-zero elements

$$g^{rr} = 1, \quad g^{\theta_p\theta_p} = \frac{1}{r^2}, \quad g^{\phi\phi} = \frac{1}{R^2}, \tag{4.8}$$

and the Jacobian is $J = Rr$. The one-dimensional Jacobian in Eq. (4.6) is obtained integrating over θ_p and ϕ, giving $s(r) = 4\pi^2 R_0 r$. With a constant diffusion coefficient D, the old and new operators then become

$$\Delta r_{old} = \frac{1}{r}D\Delta t \pm \sqrt{2D\Delta t}, \tag{4.9}$$

$$\Delta r_{new} = \left(1 + \frac{\cos\theta_p}{\frac{R_0}{r} + \cos\theta_p}\right)\frac{1}{r}D\Delta t \pm \sqrt{2D\Delta t} \tag{4.10}$$

In the cylindrical limit, with large aspect ratio $R_0/r \gg 1$, the cosine terms in the new model can be safely ignored and the old model is recovered. However, in a tokamkak with finite aspect ratio, neglecting the cosine terms would lead to particle density that does not obey the diffusion equation (4.1). The purpose of the publication was thus to show explicitly, that care should be taken when applying anomalous diffusion in test particle simulations, and that the model presented in [51] should no longer be used.

4.2 MHD modes for fast ion transport studies

Energetic particles play a significant role in providing heating and current drive in reactor-scale tokamak plasmas [52, 53, 54], but they can

also drive magnetohydrodynamical (MHD) instabilities like Alfvén Eigenmodes (AEs) [17, 18, 19]. These instabilities act back on the energetic particles, resulting in transport of particles and energy. Studies investigating the redistribution of energetic ions in the presence of toroidal AEs (TAEs) and neoclassical tearing modes (NTMs) have been carried out but, typically, they have suffered of limitations: the studies on wave-particle interaction using orbit-following codes are either restricted to the main plasma, and to an axisymmetric magnetic background [55], or to the time-independent approximation of the slowly rotating modes, like the neoclassical tearing modes (NTMs) [56]. Calculation of fast ion power loads on PFCs, however, requires accurate modelling of the background magnetic field and particle following beyond all the way to the wall.

In Publication II, a model is developed to overcome these limitations. The paper introduces a method that facilitates combining time-dependent MHD modes and a realistic 3D magnetic field, yet allowing orbit-following up to the first wall with either guiding-center or full-orbit formalism. The model considered in Publication II mimics the actual helical nature of the MHD modes that appear on some of the so-called resonant magnetic surfaces where the field line itself after n rotations to toroidal direction and m rotations in poloidal direction. The model uses a similar parametrization as earlier works [39, 57] but, instead of relying on the straight field-line coordinates in orbit-following, the equations of motion are expressed in general Cartesian or curvilinear coordinates.

The modes are introduced as perturbations in the magnetic vector potential and in the electric scalar potential, and the perturbations are included into the particle's Hamiltonian motion by adding the magnetic perturbation into the symplectic part of both the particle and guiding center Lagrangian, and the electric perturbation into the Hamiltonian. Following the earlier approaches, the perturbation in the magnetic vector potential is taken to be parallel to the unperturbed magnetic field, i.e., $\tilde{\mathbf{A}} = \alpha(\mathbf{x}, t)\mathbf{B}$. This corresponds to a perturbation in the radial direction, as in low-β Alfvén waves or NTMs. If the helical structure of the magnetic perturbation is rotating, an electric perturbation $\tilde{\Phi}$ is induced according to the Maxwell's equations. This is the case for fast rotating modes, such as TAEs. Typically the perturbation parameters α and $\tilde{\Phi}$ are decomposed into terms consisting of a product of a radial profile and a rotating angular

part:

$$\alpha = \sum_{nm} \alpha_{nm}(\psi_p) \sin\left(n\phi - m\theta - \omega_n t\right), \tag{4.11}$$

$$\tilde{\Phi} = \sum_{nm} \tilde{\Phi}_{nm}(\psi_p) \sin\left(n\phi - m\theta - \omega_n t\right), \tag{4.12}$$

where ψ_p is the radial flux surface coordinate (the poloidal magnetic flux), and θ and ϕ are the poloidal and toroidal angle variables, respectively. The definitions for the angles may vary depending on the implementation.

The radial profiles are particular to each (m,n)-mode. They can be given by purely theoretical expressions [58], theory-motivated parametrizations [59] or numerical estimates [55], and they define the amplitude of the perturbed fields. Thus, regardless of the method for obtaining the radial profiles, the profiles should be adjusted so that the resulting error fields match the experimental observations. The perturbation causes an island-like structures to the magnetic field line and the width of these islands can be measured by, e.g., ECE imaging, and they are proportional to the square root of the perturbation amplitude. In addition to the main island located at the resonance surface, there will be a multitude of harmonic resonances with smaller island widths. Also the widths and locations of these islands can be deduced from the experiments, helping to restrict the set of valid parameter values. Moreover, the perturbation amplitude can be measured by magnetic pick-up coils.

To demonstrate that the method presented in Publication II produces island structures that mimic the structures of the MHD modes, low-energy test particles (1 keV protons) with velocities parallel to the magnetic field were traced in the presence of NTM perturbations. The Poincaré plot of the test particle orbits in the presence of (m,n)-modes (3,2), (2,1), and (3,1) is presented in Figs 4.1. The structures of each mode are clearly visible, as are some harmonics appearing closer to separatrix.

For a comparison to the previous methods, a separate study was conducted where the perturbation field was evaluated beforehand and tabulated into the magnetic background input file. The resulting Poincaré plot is presented in Fig. 4.2, and one can conclude that no visible difference appears between the new and old methods. In Publication II, also the time-dependent model for TAEs was tested out and benchmarked to an axisymmetric code HAGIS [57]. The results agreed well.

Unlike previous approaches, the work presented in Publication II easily accommodates to non-axisymmetric magnetic fields (toroidal ripple, external coils, TBM's etc). Later, in this thesis, the model is used for estimating

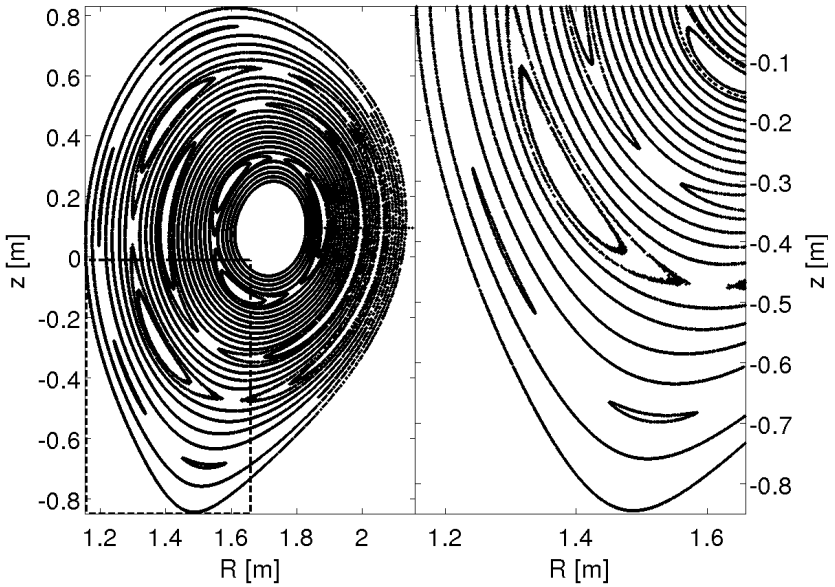

Figure 4.1. A Poincaré plot of test particle orbits in the presence of NTMs. The perturbation is implemented according to the method described in Publication II and the particle orbits are calculated using cylindrical coordinates.

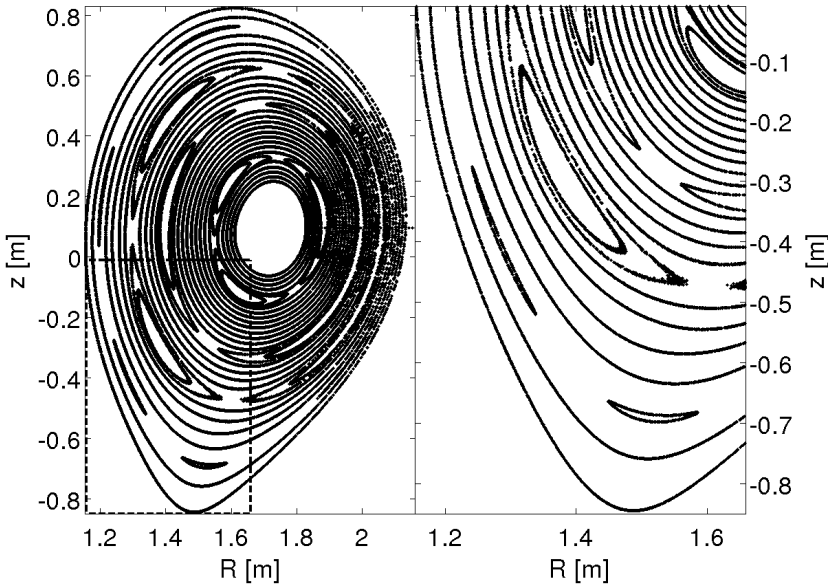

Figure 4.2. A Poincaré plot of test particle orbits in the presence of NTMs. The perturbation is evaluated before hand and added to the magnetic background input file. Hardly any differences can be found compared Fig. 4.1.

the alpha-particle transport in ITER due to relevant MHD activity. Before such a, a complete tool for solving the distribution function has to be developed.

4.3 ASCOT: a tool to solve the kinetic equation

In chapter two, the connection between a kinetic Fokker-Planck equation and a stochastic differential equation was established. This connection guarantees that following the trajectories of test particles or guiding centers according to the corresponding stochastic differential equations offers a solution to the kinetic Fokker-Planck equation, and that the solution is the statistical average of the phase space trajectories. The newest version of ASCOT code, which is described in detail in Publication IV, does exactly this. It numerically integrates the stochastic trajectories and records the paths into a multidimensional grid, thus, solving the distribution function for the minority population.

Although based on the very first principles, the code is highly sophisticated one. Engineering-wise, it has a cabability of handling a full 3-D magnetic field, and the simulation regime is typically limited by a surface constructed from triangular or quadrilateral elements representing the first wall of the tokamak device. These features allow accurate modeling of the magnetic field and the wall which both are crucial if one is interested in, for example, estimating fast ion power loads on the first wall: Local perturbations in the magnetic field affect the orbit losses, and protruding structures on the wall are more vulnerable to heat flux from plasma than the elements further away. In Figs. 4.3(a) and 4.3(b) that present the fast ion power load in ITER for both purely axisymmetric and 3-D toroidally rippled magnetic field, the importance of accurately modelling the magnetic field and wall becomes obvious. The detailed description of the wall was also one of the main features that lead to the discoveries published in [60, 61].

Regarding pure computational power, ASCOT solves a problem that has practically ideal multiprocessor scalability. Because the test particles or guiding centers do not interact with each other, each of them can be simulated by harnessing the power of one core completely. Typically, studies conducted with the code run with 2^8–2^{15} cores. More can be used if available but the code can run also with just one core on a regular desktop. Support exists for two complementary mechanisms for executing paral-

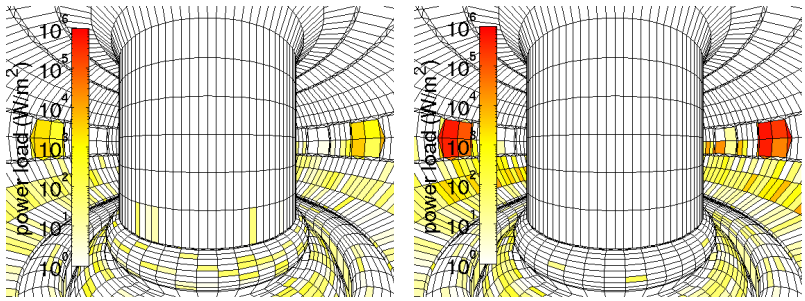

Figure 4.3. A plot of the alpha-particle power load on the first wall elements in ITER old scenario 4 with an axisymmetric magnetic field (left) and with the toroidal ripple included (right). Notice the different colors on the limiter tiles between the two figures.

lel work, one for high performance computing (HPC) via MPI [62] and another for high throughput computing (HTC) via HTCondor distributed computing software [63]. The former is used in the supercomputer environment, while the latter exploits idling workstations.

Theorywise, the code stands out from the rest. The conventional way of solving the kinetic equation including collisional effects is not the one presented in Chapters 2 and 3 in this thesis. The guiding center transport studies (see, e.g., Refs. [9, 10, 51, 64, 65, 66, 65] to mention some) typically apply a collision operator that has not been transformed to the guiding center phase space and, strictly speaking, is valid only for the particle phase space. This automatically leads to the loss of the spatial transport that arises when the transformation to guiding center phase space is done. It is also common to use different phase space coordinates for the Hamiltonian and collisional parts when solving the kinetic equation with stochastic methods, although it was explicitly shown in Chapters 2 and 3 that both the Hamiltonian and collisional motion contribute to the very same phase space coordinates. In the new version of ASCOT, the kinetic equation is solved by the book using the methods summarized in this thesis.

As the code is often used to gather information from fast ions, it has an in-built capability to initialize test particles that represent the actual particles. The sources include energetic ions and neutrons from fusion reactions, as well as ions generated by neutral beam injection (NBI) or ion cyclotron resonance heating (ICRH). The fusion product source is calculated according to the densities of the reacting particle species and cross sections provided by Bosch and Hale [67]. Four different reactions have

been implemented: D(d,n)^{3}He, D(d,p)T, T(d,n)α and ^{3}He(d,P)α. The model for the NBI source is beamlet-based and, to generate an NBI test particle, a neutral particle from a random beamlet is chosen and assigned a velocity in the direction of the beamlet, offset by a usually bi-gaussian dispersion. The neutral is then advanced along its velocity vector until it either hits an obstacle or gets ionized. In the ionization location, a test particle is recorded. The NBI model is benchmarked and will be published later. Accurate modeling of the ICRH ions would require self-consistent simulations taking into account the wave field caused by the ICRH antenna and its interaction with the plasma [68, 69, 70, 71, 72]. The ICRH ion source model in ASCOT, however, is an approximation where the ICRH accelerated ions are obtained assuming that the distribution of ICRH ions is peaked roughly at the magnetic axis with a finite half-width responsible for spreading in the radial coordinate ψ_p . In addition, the ICRH ions will have the banana turning points at places where the frequency of the ICRH wave, ω, meets the resonance condition, $\omega = n\Omega$, for the nth harmonic of the wave field. As Ω is proportional to the magnetic field B, which is roughly a function of the inverse major radius $1/R$, this creates an additional condition, and the ICRH distribution will be roughly limited to certain resonant major radius rather than spreading freely in ψ_p.

ASCOT can be used also for modelling impurity transport. The code has been applied to, e.g., simulating trace element injection experiments [60, 61]. In contrast to fast particles, however, impurities in the SOL have typically very low energies (of the order of 1–100 eV). As typical flow velocities of Mach 0.5–1 have been measured in the SOL region of various tokamaks [73], the flows have significant effect on the long range transport of the low energy impurities. Additionally, the charge state of impurity particles can change significantly during simulations, which further affects their transport. Thus, the code has been enhanced to include also a model for plasma flows and for effective ionization and recombination according to the reaction rates imported from the ADAS database [74]. At the time of writing, data for carbon, beryllium, tungsten and nitrogen have been imported into the code.

Though the primary task for the code is to produce the minority particle distribution function, it provides the user also with various moments of the actual distribution. These moments are recorded during the simulation and can have up to six dimensions. Dimensions common to all are *time* and *test particle species*. The remaining are used for the desired

phase space coordinates or quantities. The most important profiles available include the particle density, energy density, parallel energy density, parallel current, toroidal current, collisional power deposition, collisional torque deposition, and toroidal $j \times B$ torque. The collisional power and torque depositions depending on the interactions with the background are produced separately for each background species. For compatibility with the 1-D transport codes, any distribution can be produced as a function of the radial coordinate ψ_p or, alternatively, in a cylindrical (R, z)-grid, and the actual distribution function is available in four phase space dimensions $(R, z, \mathrm{v}_\parallel, \mathrm{v}_\perp)$ or (R, z, ξ, E), where $\xi = v_\parallel / v$ is the pitch-angle cosine. An example of an NBI slowing down distribution function is shown in Fig. 4.4.

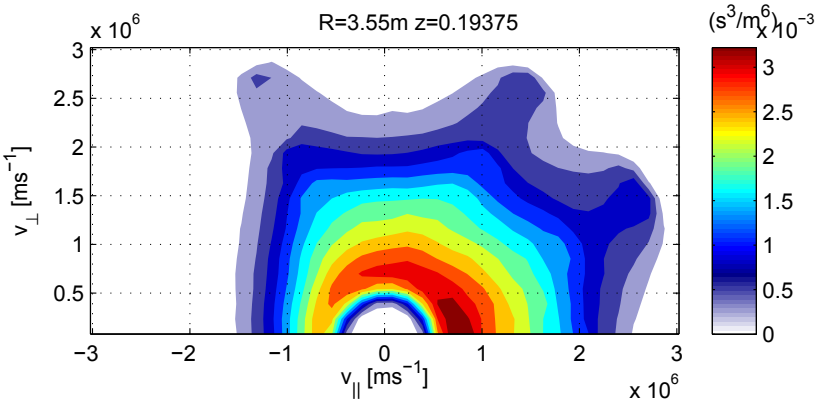

Figure 4.4. An example of an NBI slowing-down distribution function produced by ASCOT for a JET-like tokamak. One spatial position ($R = 3.55, z = 0.19375$) at outer midplane was chosen for presenting the structure of the velocity space.

The older version of the code had been used in various tasks [75, 76, 77, 78, 79] and, especially, to estimate the fast ion transport in ITER [11, 12, 13]. As the new code includes also the model for accounting the effects of MHD modes, the modes ITER is known to be prone to, it can be used to complement the previous studies for ITER to estimate the fast ion transport resulting from an interplay between 3-D magnetic field and MHD activity. Next, such an application of the new ASCOT code is presented and the results summarized.

4.4 Transport of alpha-particles in ITER under MHD activity

Gorelenkov and White have recently studied the effect of TAEs in ITER on both fusion alphas and NBI ions [80]. The analysis, however, was limited inside the main plasma, which can lead to overestimating the losses as some of the particles will re-enter the plasma. Their model for the toroidal ripple was an analytic fit to data, neglecting the ferritic inserts (FIs) and test blanket modules (TBMs). Very similar work was done also by Van Zeeland *et al* [81] to study the effect of TAEs in both DIII-D and ITER. Also this study neglected the details of 3D magnetic field. The effect of the local perturbations, however, can be significant [11, 12, 13] and, thus, a study including both the MHD activity (NTMs and TAEs) and the effects of FIs and TBMs was found necessary.

The detailed results of this study are presented in Publication V and here only main observations are reviewed. The effect of the NTMs on the alpha particles was studied in the 15 MA H-mode scenario, including both (3,2) and (2,1) modes, one at a time. The NTMs were assumed stationary as the rotation frequency is low. The effect of TAEs was studied in the 9 MA advanced scenario, concentrating on the most unstable mode $n = 5$. The eigenfunctions (the radial profiles) for the various poloidal mode numbers were calculated by the LIGKA code [82], and the frequency of the mode was 51.5 kHz.

Since efficient means to reduce the sizes of the NTMs have been developed [83, 84], the most important NTM-related question to be addressed was how large the perturbation amplitude could be if the wall power load density was to remain within the design limits [85], i.e., within 0.5 MW/m^2 on the main the wall and 20 MW/m^2 in the divertor area. First, scanning the total alpha particle wall power load as a function of the perturbation amplitude, a strong correlation was found, as illustrated in figures 4.5(a) and 4.5(b). Even with the largest perturbation amplitude, however, the wall power load densities (see Fig. 5 in Publication V) where found to remain within the design limits. In fact, if one is to use ECCD as a tool to mitigate the NTMs, the relevant operation regime would be $\delta B/B < 0.75 \cdot 10^{-2}$ confirming that the NTMs should not pose a threat to the integrity of the PFCs from the alpha particle point of view.

The study of TAEs supported the earlier studies [80, 81], revealing that the wall power load would not be increased significantly compared to the MHD quiescent case. It should be noted, though, that in Publication V

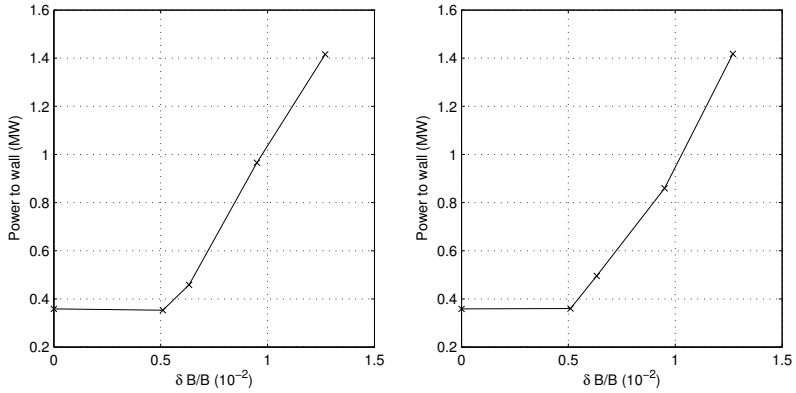

Figure 4.5. The total alpha particle wall power load vs. perturbation amplitude for a) the (3,2) NTM, and b) the (2,1) NTM. As the NTMs are expected to be mitigated in ITER, the relevant operation region will correspond to the first three bullets.

only one toroidal mode and amplitude was used in the simulations, and that the mode selected was the most unstable from the MHD point of view. It, however, might not be the most detrimental one considering the fast ion confinement.

Although no significant effect from TAEs on the wall power load was found, redistribution inside the plasma was observed. The relative difference in alpha particle density with and without the $n = 5$ TAEs is presented in Fig. 4.6(a). Side by side with the change in the density, the magnetic field perturbation strength in Fig. 4.6(b) reveals a clear correlation between the transport and the mode structures: the modes appear to push a portion of the alpha particles outwards from the very core of the plasma. More importantly, the specific shape of the red region in Fig. 4.6(a) suggests that the density increase could be a result of increase especially in the passing particles. To verify the assumption, the velocity space distribution is presented in Fig. 4.7 and, indeed, particles are found to experience transport from trapped to passing ones.

As the total plasma density is much higher than the density of fusion products, even changes of up to 10 % in the alpha particle density do not sound alarming considering the total density. The redistribution of alpha particles especially in the core region, however, directly affects also the alpha heating profile. In Publication V, the power to plasma provided by alphas was observed to reduce up to 10 % in the core, and similar increase was observed a bit further away from the core mimicking the density changes in Fig. 4.6(a). In ITER, the alpha particles are assumed to provide a significant amount of the total heating power and, therefore,

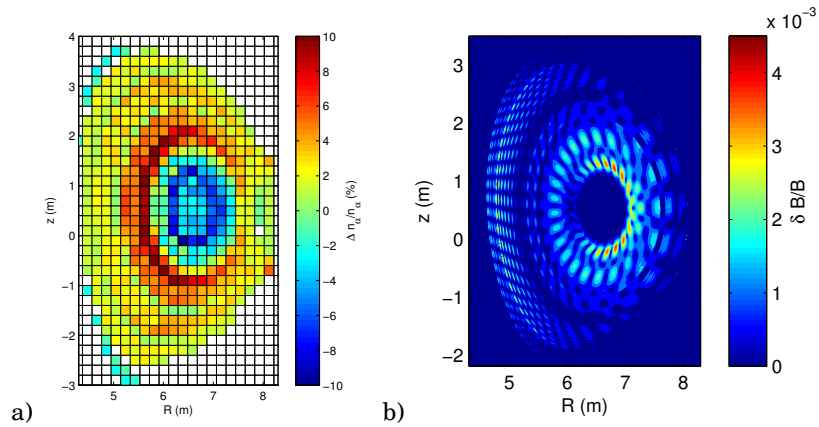

Figure 4.6. (a) The relative change in the simulated alpha particle density brought about by the $n = 5$ TAE modes. (b) A 2D map of the magnetic perturbation strength given as a fraction of the background magnetic field strength. A clear correlation between (a) and (b) is observed.

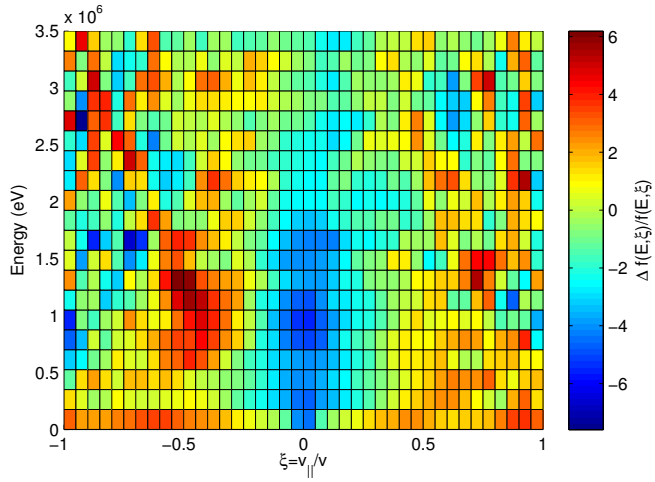

Figure 4.7. The relative difference of the histogram showing the particle pitch and energy for the slowing down time with and without the n=5 TAE. There is a clear velocity-space redistribution from trapped to passing particles.

such a change in the power deposition could lead to local changes in the temperature profile. The change in the temperature profile would then affect the source of the fusion products and possibly also the spectrum of the MHD modes excited by the fusion products. The results presented in Publication V thus suggest that a more precise investigations, preferably self-consistent ones, should be initiated on this matter.

5. Summary and future prospects

In this thesis, the basic theory behind Monte Carlo simulations of minority populations in tokamak plasmas was discussed at a rather detailed level. In the beginning of chapter 2, an explicit proof of the connection between stochastic processes and the kinetic Fokker-Planck equation was presented to offer a method for solving the kinetic equation in terms of Monte Carlo simulations. In the end of chapter 2, the necessary expressions to address the kinetic equation of charged particles were given.

Chapter 3 then continued the theoretical treatment by introducing the guiding center formalism that can be used to eliminate the fast gyromotion from the particle kinetic equation. Since the derivation of the guiding center theory is typically not addressed in dissertations, it was decided that the discussion should proceed in a detailed level. In particular, because the stochastic differential equation describing both the Hamiltonian and collisional motion of a guiding center was derived for the first time in Publication III, the details of the most important steps were given explicitly. Together, the chapters 2 and 3 now provide a solid consistent theoretical basis for anyone interested in the minority particle studies.

The basic theory was then replenished in Chapter 4 with models for anomalous diffusion and MHD modes presented in Publications I and II and, finally, applied to conduct a numerical study of fusion born alpha particles in ITER with the tool develop in Publication IV. The results from the study were presented in Publication V and confirmed that the redistribution caused by neoclassical tearing modes would not comprimise the integrity of the plasma facing components, if the modes are mitigated early enough. The study, however, pointed out that more thorough investigations of the effects of Alfvén Eigenmodes should be carried out. The observed redistribution of alphas in the plasma core changes the power deposition to the main plasma and affects the internal heating mecha-

nism. As ITER is to demonstrate the feasibility of fusion produced energy on Earth, every megawatt of lost heating power makes the goal more difficult to achieve. Therefore, it should be verified that the change in the alpha heating power caused by the modes would not lead to further alpha transport: If the heating power changes according to the results presented in Publication V the temperature profile could experience a similar change, and a part of the alphas now born in the very core of the plasma would be born further away from the core. The change in the fast alpha population could then change the spectra of the excited MHD modes which could, in turn, push the alphas even further out from the core. Future studies are thus needed to confirm that this cycle would not happen.

A. Exterior calculus on differential forms

A differential form ω_k of the order k, referred to as k-form, is defined

$$\omega_k = \frac{1}{k!}\omega_{i_1,i_2,\ldots,i_k}\mathrm{d}z^{i_1}\wedge\mathrm{d}z^{i_1}\wedge\ldots\wedge\mathrm{d}z^{i_k}, \tag{A.1}$$

where d denotes the exterior derivative, $\omega_{i_1,i_2,\ldots,i_k}$ is antisymmetric and $\wedge$ is the wedge product. The wedge product, being a generalization of a cross product $\times$, is *skew commutative*: A wedge product of a k-form ω_k and an l-form Ω_l satisfies

$$\omega_k\wedge\Omega_l = (-1)^{kl}\Omega_l\wedge\omega_k, \tag{A.2}$$

and the wedge of two identical k-forms is zero

$$\omega_k\wedge\omega_k = 0. \tag{A.3}$$

A scalar field $f(\mathbf{z})$ is an example of a 0-form and the differential of the scalar field, $\mathrm{d}f = \partial_\alpha f\mathrm{d}z^\alpha$, is an example of a 1-form. Thus, for example, the differential of a Lagrangian action clearly is a one-form.

The exterior derivative of a differential form is constructed using the identity $\mathrm{d}^2 = 0$, the product rule for a k-form ω_k and an l-form Ω_l

$$\mathrm{d}\left(\omega_k\wedge\Omega_l\right) = \left(\mathrm{d}\omega_k\right)\wedge\Omega_l + (-1)^k\omega_k\wedge\left(\mathrm{d}\Omega_l\right), \tag{A.4}$$

and the exterior derivative of a one-form

$$\begin{aligned}\mathrm{d}\left(\omega_\alpha\mathrm{d}z^\alpha\right) =& \mathrm{d}\omega_\alpha\wedge\mathrm{d}z^\alpha\\ =& \partial_\beta\omega_\alpha\mathrm{d}z^\beta\wedge\mathrm{d}z^\alpha\\ =& \frac{1}{2}\left(\partial_\alpha\omega_\beta - \partial_\beta\omega_\alpha\right)\mathrm{d}z^\alpha\wedge\mathrm{d}z^\beta.\end{aligned} \tag{A.5}$$

Using these expressions it is then possible to calculate the exterior derivative of any differential form. The property that the second exterior derivative, d^2, of any k-form, ω_k, is zero, can be most easily demonstrated for a

zero-form by direct calculation

$$\mathrm{d}f = \partial_\alpha f \mathrm{d}z^\alpha \tag{A.6}$$

$$\mathrm{d}^2 f = \frac{1}{2}\left(\partial^2_{\alpha\beta} f - \partial^2_{\beta\alpha} f\right) \mathrm{d}z^\alpha \wedge \mathrm{d}z^\beta = 0, \tag{A.7}$$

and, in a three dimensional space, this corresponds to the identity $\nabla \times \nabla f = 0$.

The contraction operator $i_{\boldsymbol{G}}$ defined with a vector field $\boldsymbol{G}$, is a generalization of a directional derivative. Operating on a k-form, the contraction reduces the order to $(k-1)$. The contraction of a wedge product of a k-form ω_k and an l-form Ω_l is defined by

$$i_{\boldsymbol{G}} \cdot (\omega_k \wedge \Omega_l) = (i_{\boldsymbol{G}} \cdot \omega_k) \wedge \Omega_l + (-1)^k \omega_k \wedge (i_{\boldsymbol{G}} \cdot \Omega_l), \tag{A.8}$$

and given the contraction of a one-form according to

$$i_{\boldsymbol{G}} \cdot \omega_1 = i_{\boldsymbol{G}} \cdot (\omega_\alpha \mathrm{d}z^\alpha) \tag{A.9}$$

$$= G^\alpha \omega_\alpha, \tag{A.10}$$

the operation $i_{\boldsymbol{G}} \cdot \omega_k$ can be constructed iteratively. One should note that the contraction of a zero form is zero.

The Lie-derivative of a k-form ω_k is calculated according to the Cartan identity

$$\mathcal{L}_{\boldsymbol{G}} \omega_k = i_{\boldsymbol{G}} \cdot \mathrm{d}\omega_k + \mathrm{d}\left(i_{\boldsymbol{G}} \cdot \omega_k\right). \tag{A.11}$$

Thus, the Lie-derivative of a scalar field is simply the contraction of the related one-form according to

$$\mathcal{L}_{\boldsymbol{G}} f = i_{\boldsymbol{G}} \cdot \mathrm{d}f = G^\alpha \partial_\alpha f \tag{A.12}$$

and the Lie-derivative of a one-form $\omega_1 = \omega_\alpha \mathrm{d}z^\alpha$, needed in this thesis, is given by

$$\mathcal{L}_{\boldsymbol{G}} \omega_1 = G^\beta \left(\partial_\beta \omega_\alpha - \partial_\alpha \omega_\beta\right) \mathrm{d}z^\alpha + \mathrm{d}\left(G^\alpha \omega_\alpha\right). \tag{A.13}$$

For example, in a three dimensional space with $\omega_1 = \mathbf{C} \cdot \mathrm{d}\mathbf{X}$, the Lie derivative is

$$\mathcal{L}_{\boldsymbol{G}} \omega_1 = -\boldsymbol{G} \times \nabla \times \mathbf{C} \cdot \mathrm{d}\mathbf{X} + \mathrm{d}\left(\boldsymbol{G} \cdot \mathbf{C}\right). \tag{A.14}$$

Bibliography

[1] M Keilhacker, G Becker, K Bernhardi, A Eberhagen, M ElShaer, G FuBmann, O Gehre, J Gernhardt, G v Gierke, E Glock, G Haas, F Karger, S Kissel, O Kluber, K Kornherr, K Lackner, G Lisitano, G G Lister, J Massig, H M Mayer, K McCormick, D Meisel, E Meservey, E R Muller, H Murmann, H Niedermeyer, W Poschenrieder, H Rapp, B Richter, H Rohr, F Ryter, F Schneider, S Siller, P Smeulders, F Soldner, E Speth, A Stabler, K Steinmetz, K-H Steuer, Z Szymanski, G Venus, O Vollmer, and F Wagner. Confinement studies in L and H-type Asdex discharges. *Plasma Physics and Controlled Fusion*, 26(1A):49–63, January 1984.

[2] E. J. Doyle, R. J. Groebner, K. H. Burrell, P. Gohil, T. Lehecka, Jr. N. C. Luhmann, H. Matsumoto, T. H. Osborne, W. A. Peebles, and R. Philipona. Modifications in turbulence and edge electric fields at the L–H transition in the DIII-D tokamak. *Physics of Fluids B: Plasma Physics*, 3(8):2300–2307, August 1991.

[3] J. Stober, M. Maraschek, G.D. Conway, O. Gruber, A. Herrmann, A.C.C. Sips, W. Treutterer, H. Zohm, and ASDEX Upgrade Team. Type II ELMy H modes on ASDEX Upgrade with good confinement at high density. *Nuclear Fusion*, 41(9):1123–1134, September 2001.

[4] W Suttrop. The physics of large and small edge localized modes. *Plasma Physics and Controlled Fusion*, 42(5A):A1–A14, 2000.

[5] W. Suttrop, T. Eich, J.C. Fuchs, S. Günter, A. Janzer, A. Herrmann, A. Kallenbach, P. T. Lang, T. Lunt, M. Maraschek, R. M. McDermott, A. Mlynek, T. Pütterich, M. Rott, T. Vierle, E. Wolfrum, Q. Yu, I. Zammuto, H. Zohm, and the ASDEX Upgrade Team. First observation of edge localized modes mitigation with resonant and nonresonant magnetic perturbations in asdex upgrade. *Phys. Rev. Lett.*, 106:225004, 2011.

[6] W Suttrop, L Barrera, A Herrmann, R M McDermott, T Eich, R Fischer, B Kurzan, P T Lang, A Mlynek, T Pütterich, S K Rathgeber, M Rott, T Vierle, E Viezzer, M Willensdorfer, E Wolfrum, I Zammuto, and the ASDEX Upgrade Team. Studies of edge localized mode mitigation with new active in-vessel saddle coils in asdex upgrade. *Plasma Physics Controlled Fusion*, 53(12):124014, 2011.

[7] K. Shinohara, T. Kurki-Suonio, D. Spong, O. Asunta, K. Tani, E. Strumberger, S. Briguglio, T. Koskela, G. Vlad, S. Günter, G. Kramer, S. Putvinski, K. Hamamatsu, and ITPA Topical Group on Energetic Particles. Effects

of complex symmetry-breakings on alpha particle power loads on first wall structures and equilibrium in ITER. *Nuclear Fusion*, 51(6):063028, 2011.

[8] K. Tani, K. Shinohara, T. Oikawa, H. Tsutsui, S. Miyamoto, Y. Kusama, and T. Sugie. Effects of ELM mitigation coils on energetic particle confinement in ITER steady-state operation. *Nuclear Fusion*, 52(1):013012, 2012.

[9] K. Shinohara, K. Tani, T. Oikawa, S. Putvinski, M. Schaffer, and A. Loarte. Effects of rippled fields due to ferritic inserts and ELM mitigation coils on energetic ion losses in a 15 MA inductive scenario in ITER. *Nuclear Fusion*, 52(9):094008, 2012.

[10] K. Tani, K. Shinohara, T. Oikawa, H. Tsutsui, S. Miyamoto, Y. Kusama, and T. Sugie. Effects of elm mitigation coils on energetic particle confinement in iter steady-state operation. *Nuclear Fusion*, 52(1):013012, 2012.

[11] T. Kurki-Suonio, O. Asunta, T. Hellsten, V. Hynönen, T. Johnson, T. Koskela, J. Lönnroth, V. Parail, M. Roccella, G. Saibene, A. Salmi, and S. Sipilä. ASCOT simulations of fast ion power loads to the plasma-facing components in ITER. *Nuclear Fusion*, 49(9):095001, 2009.

[12] T. Kurki-Suonio, O. Asunta, E. Hirvijoki, T. Koskela, A. Snicker, T. Hauff, F. Jenko, E. Poli, and S. Sipilä. Fast ion power loads on ITER first wall structures in the presence of NTMs and microturbulence. *Nuclear Fusion*, 51(8):083041, 2011.

[13] A. Snicker, S. Sipilä, and T. Kurki-Suonio. Orbit-following fusion alpha wall load simulation for ITER scenario 4 including full orbit effects. *Nuclear Fusion*, 52(9):094011, 2012.

[14] JET Team (prepared by G.T.A. Huysmans). Observation of neoclassical tearing modes in JET. *Nuclear Fusion*, 39(11Y):1965, 1999.

[15] R J Buttery, S Günter, G Giruzzi, T C Hender, D Howell, G Huysmans, R J La Haye, M Maraschek, H Reimerdes, O Sauter, C D Warrick, H R Wilson, and H Zohm. Neoclassical tearing modes. *Plasma Physics and Controlled Fusion*, 42(12B):B61, 2000.

[16] M. García-Muñoz, P. Martin, H.-U. Fahrbach, M. Gobbin, S. Günter, M. Maraschek, L. Marrelli, H. Zohm, and the ASDEX Upgrade Team. Ntm induced fast ion losses in asdex upgrade. *Nuclear Fusion*, 47(7):L10–L15, July 2007.

[17] G. Y. Fu, R. Nazikian, R. Budny, and Z. Chang. Alpha particle-driven toroidal alfvén eigenmodes in tokamak fusion test reactor deuterium–tritium plasmas: Theory and experiments. *Physics of Plasmas (1994-present)*, 5(12):4284–4291, 1998.

[18] C.Z Cheng, Liu Chen, and M.S Chance. High-n ideal and resistive shear alfvén waves in tokamaks. *Annals of Physics*, 161(1):21 – 47, 1985.

[19] W. W. Heidbrink, E. J. Strait, M. S. Chu, and A. D. Turnbull. Observation of beta-induced alfvén eigenmodes in the diii-d tokamak. *Phys. Rev. Lett.*, 71:855–858, Aug 1993.

[20] J. D. Huba. NRL Plasma Formulary. Naval Research Laboratory, Washington, D.C., 2006.

[21] J D Lawson. Some criteria for a power producing thermonuclear reactor. *Proceedings of the Physical Society. Section B*, 70(1):6, 1957.

[22] R.B. White. *The Theory of Toroidally Confined Plasmas*. Imperial College Press, 2006.

[23] Allan N. Kaufman. Quasilinear diffusion of an axisymmetric toroidal plasma. *Physics of Fluids (1958-1988)*, 15(6):1063–1069, 1972.

[24] Ira B. Bernstein and K. Molvig. Lagrangian formulation of neoclassical transport theory. *Physics of Fluids (1958-1988)*, 26(6):1488–1507, 1983.

[25] F. S. Zaitsev, M. R. O'Brien, and M. Cox. Three-dimensional neoclassical nonlinear kinetic equation for low collisionality axisymmetric tokamak plasmas. *Physics of Fluids B: Plasma Physics (1989-1993)*, 5(2):509–519, 1993.

[26] L.-G. Eriksson and P. Helander. Monte carlo operators for orbit-averaged fokker–planck equations. *Physics of Plasmas (1994-present)*, 1(2):308–314, 1994.

[27] V. A. Yavorskij, Zh. N. Andrushchenko, J. W. Edenstrasser, and V. Ya Goloborod'ko. Three-dimensional fokker–planck equation for trapped fast ions in a tokamak with weak toroidal field ripples. *Physics of Plasmas*, 6(10):3853–3867, 1999.

[28] J. Decker, Y. Peysson, A. J. Brizard, and F.-X. Duthoit. Orbit-averaged guiding-center fokker–planck operator for numerical applications. *Physics of Plasmas (1994-present)*, 17(11):112513, 2010.

[29] Robert G. Littlejohn. A guiding center hamiltonian: A new approach. *Journal of Mathematical Physics*, 20(12):2445–2458, 1979.

[30] Robert G. Littlejohn. Hamiltonian perturbation theory in noncanonical coordinates. *Journal of Mathematical Physics*, 23(5):742–747, 1982.

[31] Robert G. Littlejohn. Variational principles of guiding centre motion. *Journal of Plasma Physics*, 29:111–125, 2 1983.

[32] Alain J. Brizard. Nonlinear gyrokinetic vlasov equation for toroidally rotating axisymmetric tokamaks. *Physics of Plasmas (1994-present)*, 2(2):459–471, 1995.

[33] John R. Cary and Alain J. Brizard. Hamiltonian theory of guiding-center motion. *Rev. Mod. Phys.*, 81:693–738, May 2009.

[34] Theodore G. Northrop. The guiding center approximation to charged particle motion. *Annals of Physics*, 15(1):79 – 101, 1961.

[35] Theodore G. Northrop. Adiabatic charged-particle motion. *Reviews of Geophysics*, 1(3):283–304, 1963.

[36] A. I. Morozov and L. S. Solovev. The structure of magnetic fields. In M. A. Leontovich, editor, *Reviews of Plasma Physics*, volume 2, pages 1–101. Consultants Bureau, New York, 1966.

[37] H. Vernon Wong. Hamiltonian formulation of guiding center motion and of the linear and nonlinear gyrokinetic equation. *Physics of Fluids (1958-1988)*, 25(10):1811–1820, 1982.

[38] R. B. White, A. H. Boozer, and Ralph Hay. Drift hamiltonian in magnetic coordinates. *Physics of Fluids (1958-1988)*, 25(3):575–576, 1982.

[39] R. B. White and M. S. Chance. Hamiltonian guiding center drift orbit calculation for plasmas of arbitrary cross section. *Physics of Fluids (1958-1988)*, 27(10):2455–2467, 1984.

[40] Alain J. Brizard. A guiding-center fokker–planck collision operator for nonuniform magnetic fields. *Physics of Plasmas*, 11(9):4429–4438, 2004.

[41] S. Chandrasekhar. Stochastic problems in physics and astronomy. *Rev. Mod. Phys.*, 15:1–89, Jan 1943.

[42] Marshall N. Rosenbluth, William M. MacDonald, and David L. Judd. Fokker-planck equation for an inverse-square force. *Phys. Rev.*, 107:1–6, Jul 1957.

[43] A. Kolmogoroff. Über die analytischen methoden in der wahrscheinlichkeitsrechnung. *Mathematische Annalen*, 104(1):415–458, 1931.

[44] A.N. Kolmogorov. *Grundbegriffe der Wahrscheinlichkeitsrechnung*. Ergebnisse der Mathematik und Ihrer Grenzgebiete. Julius Springer, 1933.

[45] B. Øksendal. *Stochastic Differential Equations: An Introduction with Applications*. Hochschultext / Universitext. Springer, 2003.

[46] V. I. Arnold. *Mathematical Methods of Classical Mechanics, 2nd. ed.* Graduate text in mathematics. Springer-Verlag Pub. Co., 1989.

[47] H. Goldstein. *Classical mechanics*. Addison-Wesley series in physics. Addison-Wesley Pub. Co., 1980.

[48] S. Ichimaru. *Basic Principles of Plasma Physics: A Statistical Approach*. Frontiers in Physics. Benjamin, 1973.

[49] F. L. Hinton and R. D. Hazeltine. Theory of plasma transport in toroidal confinement systems. *Rev. Mod. Phys.*, 48:239–308, Apr 1976.

[50] Thibaut Vernay. *Collisions in Global Gyrokinetic Simulations of Tokamak Plasmas using the Delta-f Particle-In-Cell Approach: Neoclassical Physics and Turbulent Transport*. PhD thesis, École polytechnique fédérale de Lausanne, 2013.

[51] Allen H. Boozer and Gioietta Kuo-Petravic. Monte carlo evaluation of transport coefficients. *Physics of Fluids*, 24(5):851–859, 1981.

[52] T. Oikawa, Y. Kamada, A. Isayama, T. Fujita, T. Suzuki, N. Umeda, M. Kawai, M. Kuriyama, L.R. Grisham, Y. Ikeda, K. Kajiwara, K. Ushigusa, K. Tobita, A. Morioka, M. Takechi, T. Itoh, and JT-60 Team. Reactor relevant current drive and heating by n-nbi on jt-60u. *Nuclear Fusion*, 41(11):1575, 2001.

[53] P. R. Thomas, P. Andrew, B. Balet, D. Bartlett, J. Bull, B. de Esch, A. Gibson, C. Gowers, H. Guo, G. Huysmans, T. Jones, M. Keilhacker, R. Koenig, M. Lennholm, P. Lomas, A. Maas, F. Marcus, F. Nave, V. Parail, F. Rimini, J. Strachan, K-D. Zastrow, and N. Zornig. Observation of alpha heating in jet dt plasmas. *Phys. Rev. Lett.*, 80:5548–5551, Jun 1998.

[54] T E Stringer. Radial profile of alpha -particle heating in a tokamak. *Plasma Physics*, 16(7):651, 1974.

[55] S.D. Pinches, V.G. Kiptily, S.E. Sharapov, D.S. Darrow, L.-G. Eriksson, H.-U. Fahrbach, M. García-Muñoz, M. Reich, E. Strumberger, A. Werner, the ASDEX Upgrade Team, and JET-EFDA Contributors. Observation and modelling of fast ion loss in jet and asdex upgrade. *Nuclear Fusion*, 46(10):S904, 2006.

[56] E. Strumberger, S. Günter, E. Schwarz, C. Tichmann, and the ASDEX Upgrade Team. Fast particle losses due to NTMs and magnetic field ripple. *New Journal of Physics*, 10(2):023017 (21pp), 2008.

[57] S.D. Pinches, L.C. Appel, J. Candy, S.E. Sharapov, H.L. Berk, D. Borba, B.N. Breizman, T.C. Hender, K.I. Hopcraft, G.T.A. Huysmans, and W. Kerner. The HAGIS self-consistent nonlinear wave-particle interaction model. *Computer Physics Communications*, 111(1-3):133 – 149, 1998.

[58] Q. Yu. Numerical modeling of diffusive heat transport across magnetic islands and local stochastic field. *Physics of Plasmas*, 13(6):062310, 2006.

[59] V. Igochine, O. Dumbrajs, D. Constantinescu, H. Zohm, G. Zvejnieks, and the ASDEX Upgrade Team. Stochastization as a possible cause for fast reconnection during mhd mode activity in the asdex upgrade tokamak. *Nuclear Fusion*, 46(7):741, 2006.

[60] J. Miettunen, T. Kurki-Suonio, T. Makkonen, M. Groth, A. Hakola, E. Hirvijoki, K. Krieger, J. Likonen, S. Äkäslompolo, and the ASDEX Upgrade Team. The effect of non-axisymmetric wall geometry on 13C transport in ASDEX Upgrade. *Nuclear Fusion*, 52(3):032001, 2012.

[61] J. Miettunen, M. Groth, T. Kurki-Suonio, H. Bergsåker, J. Likonen, S. Marsen, C. Silva, and S. Äkäslompolo. Predictive ASCOT modelling of ^{10}Be transport in JET with the ITER-like wall. *Journal of Nuclear Materials*, 438, Supplement(0):S612 – S615, 2013. Proceedings of the 20th International Conference on Plasma-Surface Interactions in Controlled Fusion Devices.

[62] Message Passing Interface Forum . *MPI: A Message-Passing Interface Standard, Version 2.2*. High Performance Computing Center Stuttgart (HLRS), 2009.

[63] Douglas Thain, Todd Tannenbaum, and Miron Livny. Distributed computing in practice: the condor experience. *Concurrency - Practice and Experience*, 17(2-4):323–356, 2005.

[64] Keiji Tani, Masafumi Azumi, Hiroshi Kishimoto, and Sanae Tamura. Effect of toroidal field ripple on fast ion behavior in a tokamak. *Journal of the Physical Society of Japan*, 50(5):1726–1737, 1981.

[65] M. Tessarotto, R. B. White, and L. Zheng. Monte Carlo approach to collisional transport. *Physics of Plasmas*, 1(8):2603–2613, 1994.

[66] M. Tessarotto, R. B. White, and L. Zheng. Probabilistic approach to Monte Carlo operators. *Physics of Plasmas*, 1(8):2591–2602, 1994.

[67] H.-S. Bosch and G.M. Hale. Improved formulas for fusion cross-sections and thermal reactivities. *Nuclear Fusion*, 32(4):611, 1992.

[68] J. Hedin, T. Hellsten, L.-G. Eriksson, and T. Johnson. The influence of finite drift orbit width on ICRF heating in toroidal plasmas. *Nuclear Fusion*, 42(5):527, 2002.

[69] T. Hellsten, T. Johnson, J. Carlsson, L.-G. Eriksson, J. Hedin, M. Laxåback, and M. Mantsinen. Effects of finite drift orbit width and RF-induced spatial transport on plasma heated by ICRH. *Nuclear Fusion*, 44(8):892, 2004.

[70] M. Brambilla. Numerical simulation of ion cyclotron waves in tokamak plasmas. *Plasma Physics and Controlled Fusion*, 41(1):1–34, 1999.

[71] J.C. Wright, Jungpyo Lee, E. Valeo, Paul Bonoli, C.K. Phillips, E.F. Jaeger, and R.W. Harvey. Challenges in self-consistent full-wave simulations of lower hybrid waves. *Plasma Science, IEEE Transactions on*, 38(9):2136–2143, 2010.

[72] Martin Jucker. *Self-Consistent ICRH Distribution Functions and Equilibria in Magnetically Confined Plasmas*. PhD thesis, École polytechnique fédérale de Lausanne, 2010.

[73] Nobuyuki Asakura. Understanding the SOL flow in L-mode plasma on divertor tokamaks, and its influence on the plasma transport. *Journal of Nuclear Materials*, 363 365(0):41 – 51, 2007. Plasma-Surface Interactions-17.

[74] ADAS. Atomic data and analysis software. `http://www.adas.ac.uk/`.

[75] J. A. Heikkinen, W. Herrmann, and T. Kurki-Suonio. The effect of a radial electric field on ripple-trapped ions observed by neutral particle fluxes. *Physics of Plasmas*, 4(10):3655–3662, 1997.

[76] J. A. Heikkinen, S. K. Sipilä, and T. J. H. Pättikangas. Monte Carlo simulation of runaway electrons in a toroidal geometry. *Computer Physics Communications*, 76(2):215–230, 1993.

[77] J. A. Heikkinen and S. K. Sipilä. Power transfer and current generation of fast ions with large-k_θ waves in tokamak plasmas. *Physics of Plasmas*, 2(10):3724–3733, 1995.

[78] T. Kurki-Suonio, J. A. Heikkinen, and S. I. Lashkul. Guiding-center simulations of nonlocal and negative inertia effects on rotation in a tokamak. *Physics of Plasmas*, 14(7):072510, 2007.

[79] A. Salmi, T. Johnson, V. Parail, J. Heikkinen, V. Hynönen, T. P. Kiviniemi, T. Kurki-Suonio, and JET EFDA Contributors. Ascot modelling of ripple effects on toroidal torque. *Contributions to Plasma Physics*, 48(1-3):77–81, 2008.

[80] N N Gorelenkov and R B White. Perturbative study of energetic particle redistribution by Alfvén eigenmodes in ITER. *Plasma Physics and Controlled Fusion*, 55(1):015007, 2013.

[81] M.A. Van Zeeland, N.N. Gorelenkov, W.W. Heidbrink, G.J. Kramer, D.A. Spong, M.E. Austin, R.K. Fisher, M. García Muñoz, M. Gorelenkova, N. Luhmann, M. Murakami, R. Nazikian, D.C. Pace, J.M. Park, B.J. Tobias, and R.B. White. Alfvén eigenmode stability and fast ion loss in DIII-D and ITER reversed magnetic shear plasmas. *Nuclear Fusion*, 52(9):094023, 2012.

[82] Ph. Lauber, S. Günter, A. Könies, and S.D. Pinches. LIGKA: A linear gyrokinetic code for the description of background kinetic and fast particle effects on the MHD stability in tokamaks. *Journal of Computational Physics*, 226(1):447 – 465, 2007.

[83] R.J. La Haye, R. Prater, R.J. Buttery, N. Hayashi, A. Isayama, M.E. Maraschek, L. Urso, and H. Zohm. Cross-machine benchmarking for ITER of neoclassical tearing mode stabilization by electron cyclotron current drive. *Nuclear Fusion*, 46(4):451, 2006.

[84] H. van den Brand, M. R. de Baar, N. J. Lopes Cardozo, and E. Westerhof. Integrated modelling of island growth, stabilization and mode locking: consequences for NTM control on ITER. *Plasma Physics and Controlled Fusion*, 54(9):094003, 2012.

[85] T. Hirai, K. Ezato, and P. Majerus. ITER relevant high heat flux testing on plasma facing components. *Materials Transactions*, 46(3):412–424, 2005.

It is not the money that makes the world go round. It is the electricity that we use everyday to power the lights in our homes and our cell phones. How we produce our electricity, is the question of the century. If the polluting emissions from fossil fuels are to be cut down, new clean and safe energy sources are needed desperately.

If successful, thermonuclear fusion would solve the problem at once and for all. To make it work, a massive international experiment to demonstrate the possibility of commercially produced fusion energy, the **ITER** reactor, is currently being built in Cadarache, southern France. Before the reactor starts operating, however, modeling work is needed to verify proper operation parameters.

The theory behind the models has to be solid and waterproof. The work presented here contributes both to the theory and the models used in plasma simulations of minoriry particle populations.

ISBN 978-952-60-5559-6
ISBN 978-952-60-5560-2 (pdf)
ISSN-L 1799-4934
ISSN 1799-4934
ISSN 1799-4942 (pdf)

Aalto University
School of Science
Department of Applied Physics
www.aalto.fi

BUSINESS + ECONOMY

ART + DESIGN + ARCHITECTURE

SCIENCE + TECHNOLOGY

CROSSOVER

DOCTORAL DISSERTATIONS

Aalto-DD 16/2014